Oligosaccharides Structurally Related to E-Selectin Ligands Are Inhibitors of Neural Cell Division: Synthesis, Conformational Analysis, and Biological Activity

José M. Coterón, Kamaljit Singh, Juan L. Asensio, María Domínguez-Dalda, Alfonso Fernández-Mayoralas,* Jesús Jiménez-Barbero, and Manuel Martín-Lomas*

Grupo de Carbohidratos, Instituto de Química Orgánica, CSIC, Juan de la Cierva 3, 28006 Madrid, Spain

José Abad-Rodríguez and Manuel Nieto-Sampedro

Neural Plasticity Group, Instituto Cajal, CSIC, Avda. Doctor Arce 37, 28002 Madrid, Spain

Received October 6, 1994[⊗]

Oligosaccharides containing either the Lewis X trisaccharide fragment (3-fucosyl-*N*-acetyllactosamine) with *N*-acetylgalactosamine at the C-3 position of the galactose unit (compound **2** and the 1,6-anhydro derivative **5**) or the trisaccharide 3-fucosyllactose having *N*-acetylneuraminic and sulfate groups at the C-3 position of the galactose (**3** and **4**, respectively) have been synthesized and tested for the ability to inhibit the division of astrocytes and transformed cell lines and their conformation studied. Compounds **3** and **4** are structurally related to sulfated Lewis X and sialyl Lewis X which are known to be recognized by E-selectin. The synthesis of **2** and **5** was accomplished by an original route starting from 1,6-anhydro-β-D-mannose, while **3** and **4** were efficiently prepared from methyl β-lactoside. The conformational analysis has been carried out using NMR, molecular mechanics, and molecular dynamics. Compounds **2**–**4** were inhibitors in all cell types tested showing ID_{50} values in the μM range; however, **5** showed a marked decrease in the ID_{50} value on astrocytes emphasizing upon the importance of the relative orientation of the fucosyl unit. Tetrasaccharide **3** was the most active on astrocytes (ID_{50} = 35 μM), whereas the sulfate **4** was the best inhibitor on tumor-forming C6 glioma cells (ID_{50} = 79 μM).

Introduction

In the mammalian central nervous system (CNS), glial cell number is maintained at a steady state during adulthood and old age. Cell division normally remains more a potentiality than a frequent event.[1] This steady state is probably the consequence of the balance in the activities of glial division promoters (mitogens) and glial division inhibitors. Whereas it is well known that mitogenic polypeptides are abundant in the brain,[2] evidence for the presence in rat brain of antimitotic molecules was presented recently.[3] The structure of many mitogens is known, but purification of the inhibitors has proven difficult. We showed that they are immunologically related to blood groups and to oligosaccharidic epitopes of the epidermal growth factor receptor (EGFR).[3,4] Proliferation of astrocyte in primary culture, promoted by brain extracts, was enhanced after removal of the inhibitory activity concomitantly present with the mitogens in the brain extracts. Glial proliferation after open brain injury correlated with decrease in antimitotic activity and immunoreactivity.[3,4] Thus, we hypothesized that the inhibitor may be involved in the physiological control of glial number, and based on immunological evidence, we synthesized a series of oligosaccharidic structures as potential inhibitors.[5] The tetrasaccharide α-D-GalNac(1→3)-β-D-Gal-(1→4)-[α-L-Fuc-(1→3)]-β-D-GlcOMe (**1**, Scheme 1) was the best synthetic inhibitor. It inhibited in culture the proliferation of astrocytes, as well as that of transformed neural cell lines, showing ID_{50} (50% inhibition) values in the μM range.[5] For antimitotic activity, the presence of the fucosyl and the *N*-acetylgalactosaminyl groups in **1** appeared important. Astrocytes and neurons were viable at tetrasaccharide concentrations 10-fold higher than the ID_{50}, indicating that growth inhibition did not involve cytotoxicity. Indeed, cell death was never observed in primary cultures, even at doses of tetrasaccharide that completely blocked thymidine incorporation. Some transformed cells, however, were not viable after 24 h of exposure to the tetrasaccharide at concentrations higher than 0.5 mM.[6] Cytotoxicity for fast proliferating cells raised the possibility of using this molecule for controlling pathological cell proliferation and migration (metastasis), but synthetic compounds with higher activity were deemed necessary. Now, we report the synthesis, the conformational analysis, and the biological activity of the structurally related tetrasaccharides **2** and **3**, the sulfated trisaccharide **4**, and the 1,6-anhydro derivative **5**. Compared with **1**, glycoconjugates have *N*-acetylglucosamine instead of glucose; hence, compound **2**, containing the 3-fucosyl-*N*-acetyllactosamine epitope, may be more similar to the natural regulators of cell division. The synthesis of compound **3** was undertaken since recent biological evidence[6] indicates that the natural inhibitor contains *N*-acetylneuraminic residues. Compound **4** was synthesized since it has been

[⊗] Abstract published in *Advance ACS Abstracts,* March 1, 1995.

(1) Korr, H. In *Astrocytes*; Fedoroff, S., Vernadakis, A., Eds.; Academic Press Limited: London, 1986; Vol. 3, pp 77–127.

(2) Fenfenbrenner, M.; Labourdette, G.; Pettmann, B.; Weibel, M. In *Astrocytes*; Fedoroff, S., Vernadakis, A., Eds.; Academic Press Limited: London, 1986; Vol. 2, pp 279–290.

(3) Nieto-Sampedro, M. *Science* **1988**, *240*, 1784.

(4) Nieto-Sampedro, M.; Broderick, J. T. *J. Neurosci. Res.* **1989**, *22*, 28.

(5) Santos-Benito, F. F.; Fernández-Mayoralas, A.; Martín-Lomas, M.; Nieto-Sampedro, M. *J. Exp. Med.* **1992**, *176*, 915. Santos-Benito, F. F.; Nieto-Sampedro, M.; Fernández-Mayoralas, A.; Martín-Lomas, M. *Carbohydr. Res.* **1992**, *230*, 185.

(6) Nieto-Sampedro, M. to be published.

0022-3263/95/1960-1502$09.00/0

Scheme 1

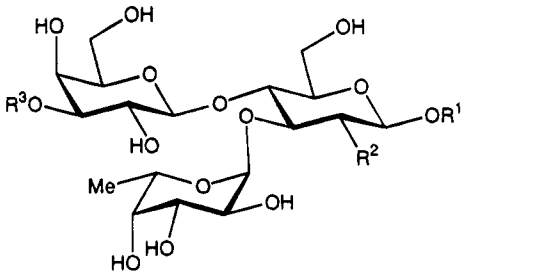

1 R^1 = Me, R^2 = OH, R^3 =

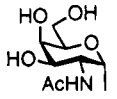

2 R^1=H, R^2 = NHAc, R^3 =

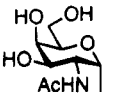

3 R^1 = Me, R^2 = OH, R^3 =

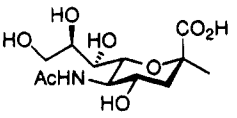

4 R^1 = Me, R^2 = OH, R^3 = SO_3H

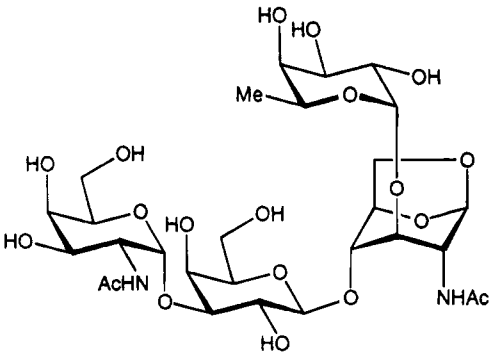

5

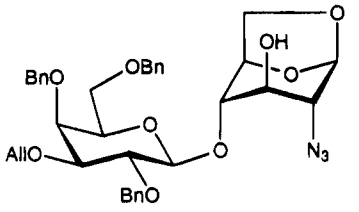

6

shown[7a] that a similarly sulfated tetrasaccharide is recognized by E-selectin with the same affinity as sialyl Lewis x (SiLe^x). Sialic acid containing glycoproteins are common in transformed cells,[8] and SiLe^x has been found in tumors[9] and in the sera of cancer patients.[10] It has been proposed that interaction of SiLe^x with the endothelial selectin ELAM-1 could mediate extravasation of tumoral cells and, hence, metastasis.[11,12] Compounds **3** and **4** present structural analogy with SiLe^x[7] and are potential ELAM-1 ligands. A preliminary account of the synthesis of **3** and **4** has been given.[13]

Results and Discussion

Synthesis of Oligosaccharides. The strategy of the synthesis of **2** was based on the preparation of the disaccharide intermediate **6**, in which HO-3 is free and HO-3′ is differently protected from the rest (Scheme 1). Sequential glycosylations and deprotections from **6** should lead to **2**. Compound **6** was prepared from 1,6-anhydro-β-D-mannopyranose derivatives, through β-galactosidation and subsequent selective transformations involving the introduction of an azide group with inversion at C-2.

Thus, β-galactosidation of 1,6-anhydro-*endo*-2,3-*O*-(4-methoxybenzylidene)-β-D-mannopyranose (**7**), obtained from 1,6-anhydro-β-D-mannopyranose following a described procedure,[14] was attempted using different galactosyl donors (Scheme 2). When **7** was condensed with benzobromogalactose (**8**)[15] under the catalysis of silver triflate with 2,6-di-*tert*-butyl-4-methylpyridine as base, the desired disaccharide **11** accompanied by its isomeric *exo*-benzylidene derivative were obtained in low yield (30%), together with the orthodisaccharide **18** (42%). With phenyl 2,3,4,6-tetra-*O*-acetyl-1-thio-β-D-galactopyranoside (**9**)[16] as donor, dimethyl(methylthio)sulfonium tetrafluoroborate as catalyst,[17] and the same base as above, compound **18** was obtained as the main product (75%). Only when the glycosidation was carried out using the donor 2,3,4,6-tetra-*O*-benzoyl-α,β-D-galactopyranosyl trichloroacetimidate (**10**)[18] and trimethylsilyl triflate as catalyst was the β-linked disaccharide derivative **11** (δ 5.08, d, 1H, $J_{1',2'}$ = 7.7 Hz, H-1′) obtained in good yield (68%).

The use of the 2,3-*O*-(4-methoxybenzylidene) protection of the 1,6-anhydro-β-D-mannopyranose residue allowed reductive cleavage in a regioselective manner.[14] Thus, treatment of **11** with sodium cyanoborohydride (25 equiv) in DMF for 24 h at room temperature in the presence of trifluoracetic acid (11 equiv) gave the alcohol **12** as the only product. Triflation of **12**, followed by treatment with sodium azide in DMF for 18 h at 0 °C gave the azide **13** in excellent yield (96%). The appearance of an intense band in the IR spectrum of **13** (2100 cm^{-1}) corroborated the presence of the azido group.

Subsequently, the transformation of the galactose unit was performed. Tetraol **14**, obtained by *O*-deacylation of **13**, was selectively allylated at the C-3′ hydroxyl using dibutyltin oxide activation[19] to afford **15** (70%), the

(7) (a) Yuen, C.-T.; Lawson, A. M.; Chai, W.; Larkin, M.; Stoll, M. S.; Stuart, A. C.; Sullivan, F. X.; Ahern, T. J.; Feizi, T. *Biochemistry* **1992**, *31*, 9126–9131. (b) Tyrrel, D.; James, P.; Rao, N.; Foxall, C.; Abbas, S.; Dasgupta, F.; Nashed, M.; Hasegawa, A.; Kiso, M.; Asa, D.; Kidd, J.; Brandley, B. K. *Proc. Natl. Acad. Sci. U.S.A.* **1991**, *88*, 10372.

(8) Warren, L.; Fuhrer, J. P.; Buck, C. A. *Proc. Natl. Acad. Sci. U.S.A.* **1972**, *69*, 1838.

(9) Fukushima, K.; Hiroto, M.; Terasaki, P. I.; Wakisaka, A. *Cancer Res.* **1984**, *44*, 5279.

(10) Iguro, T.; Wakisaka, A.; Terasaki, P. I.; Hirota, M.; Suyama, N.; Fukushima, K.; Chia, D.; Kawahara, M. *The Lancet*. **1984**, *2*, 817.

(11) Rice, G. E.; Bevilacqua, M. P. *Science*. **1989**, *246*, 1303.

(12) Walz, G.; Aruffo, A.; Kolanus, W.; Bevilacqua, M.; Seed, B. *Science* **1990**, *250*, 1132.

(13) Singh, K.; Fernández-Mayoralas, A.; Martín-Lomas, M. *J. Chem. Soc., Chem. Commun.* **1994**, 775.

(14) Kloosterman, M.; de Nijs, M. P.; van Boom, J. H. *J. Carbohydr. Chem.* **1986**, *5*, 215.

(15) Garegg, P. J.; Norberg, T. *Acta Chem. Scand., Ser. B* **1979**,*33*, 116.

(16) Ferrier, R. J.; Furneaux, R. H. *Methods Carbohydr. Chem.* **1980**, *8*, 251.

(17) Blomberg, L.; Nordberg, T. *J. Carbohydr. Chem.* **1992**, *11*, 751.

(18) Rio, S.; Beau, J.-M.; Jacquinet, J.-C. *Carbohydr. Res.* **1991**, *219*, 71.

(19) David, S.; Hanessian, S. *Tetrahedron* **1985**, *41*, 643.

Scheme 2

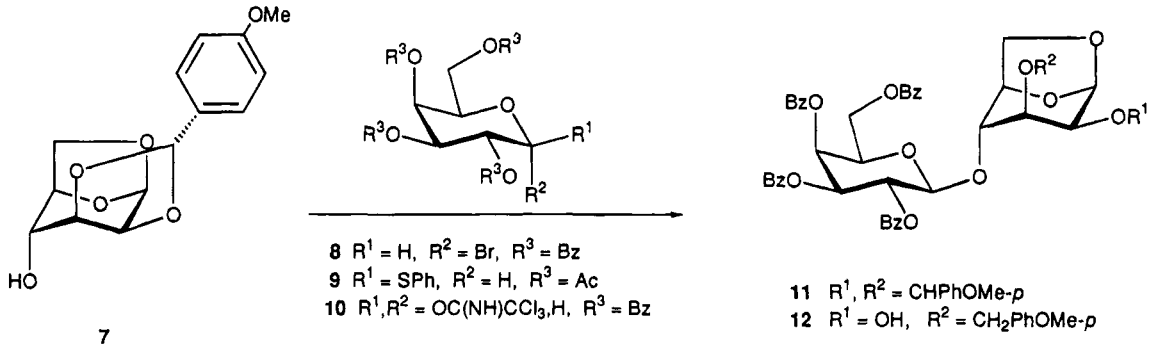

7

8 R^1 = H, R^2 = Br, R^3 = Bz
9 R^1 = SPh, R^2 = H, R^3 = Ac
10 R^1,R^2 = OC(NH)CCl_3,H, R^3 = Bz

11 R^1, R^2 = CHPhOMe-*p*
12 R^1 = OH, R^2 = CH_2PhOMe-*p*

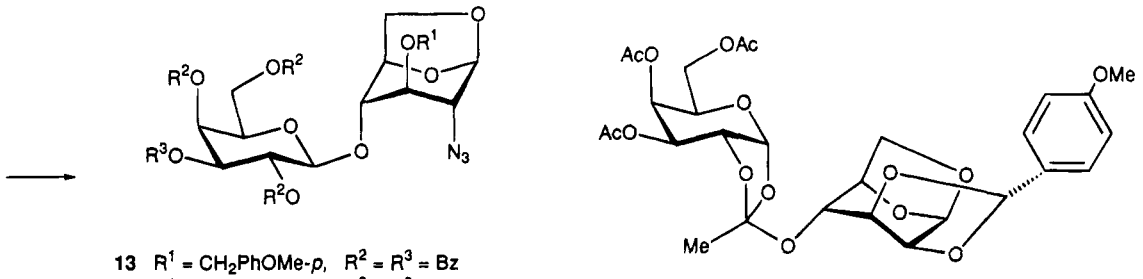

13 R^1 = CH_2PhOMe-*p*, R^2 = R^3 = Bz
14 R^1 = CH_2PhOMe-*p*, R^2 = R^3 =H
15 R^1 = CH_2PhOMe-*p*, R^2 = H, R^3 = All
16 R^1 = CH_2PhOMe-*p*, R^2 = Ac, R^3 = All
17 R^1 = CH_2PhOMe-*p*, R^2 = Bn, R^3 = All

18

Scheme 3

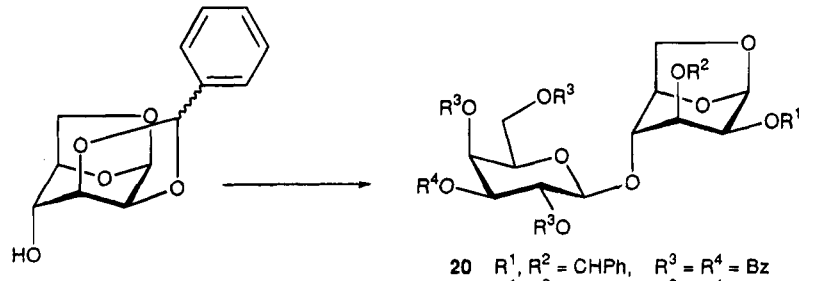

19

20 R^1, R^2 = CHPh, R^3 = R^4 = Bz
21 R^1, R^2 = CHPh, R^3 = R^4 = H
22 R^1, R^2 = CHPh, R^3 = H, R^4 = All
23 R^1, R^2 = CHPh, R^3 = Bn, R^4 = All
24 R^1 = R^2 = H, R^3 = Bn, R^4 = All

structure of which was confirmed by the ^{1}H-NMR data for the corresponding *O*-acetyl derivative **16**. Per-*O*-benzylation of **15** gave **17** (74%) which after mild hydrolysis of the *p*-methoxybenzyl group[20] in O-3 led to the disaccharide derivative **6** (78%).

This route to obtain **6** is limited by the use of a large molar excess of the toxic $NaBH_3CN$ in the reductive cleavage of **11**; however, other conventional reducing agents did not provide the desired product in a synthetically useful manner. Also, the *p*-methoxybenzyl protecting group in some intermediates was found to be labile. To circumvent these inherent limitations, a new strategy to obtain **6** was examined starting from 1,6-anhydro-2,3-*O*-benzylidene-β-D-mannopyranose[14] (**19**); in this case, the *endo*/*exo* mixture of **19** used as the synthetic sequence would not require a selective opening of benzylidene ring (Scheme 3). The β-galactosidation of **19** with the trichloroacetimidate donor as described for the glycosidation of **7** gave a higher yield of the β-linked disaccharide **20** (84%). After galactosidation we changed the strategy of the previous route, and the transformation of the galactosyl unit in **20** was first undertaken, in a similar way as described above: deacylation, regioselective allylation, and per-*O*-benzylation gave **23** through intermediates **21** and **22**. Then the benzylidene group in the mannose unit of **23** was removed with 80% acetic acid, leading to the diol **24** (92%).

The selective monotriflation at the more reactive equatorial C-2 hydroxyl of **24** and subsequent azide displacement of the triflate was attempted.[21] Compound **24** was treated with triflic anhydride (1.5 equiv) in the presence of pyridine at −40 °C until TLC analysis indicated disappearance of starting material, and then azide displacement led to the disaccharide **6** in 74% yield. This second route to **6**, involving a fewer number of steps and higher overall yield, was chosen toward the synthesis of **2** and **5**.

Glycosylation of **6** with tri-*O*-benzyl-α-L-fucopyranosyl bromide[22] promoted by mercuric bromide gave protected trisaccharide **25** (Scheme 4) with α-stereospecificity in

(20) Horita, K.; Yoshita, T.; Tanaka, T.; Oikawa, Y.; Yonemitsu, O. *Tetrahedron Lett.* **1986**, *42*, 3021.

(21) Knapp, S.; J. Naughton, A. B.; Jaramillo, C.; Pipik, B. *J. Org. Chem.* **1992**, *57*, 7328.

(22) Dejter-Juszynsky, M.; Flowers, H. M. *Carbohydr. Res.* **1971**, *18*, 219.

Scheme 4

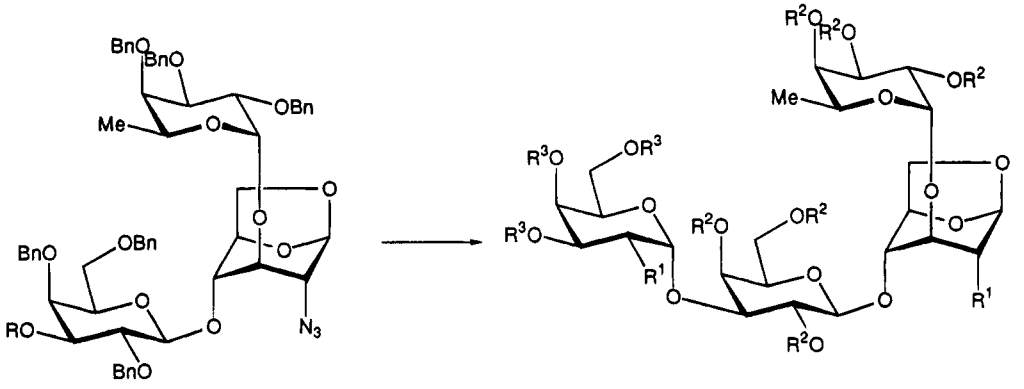

25 R = All
26 R = H

27 $R^1 = N_3$, R^2 = Bn, R^3 = Ac
28 R^1 = NHAc, $R^2 = R^3$ = Ac

Scheme 5

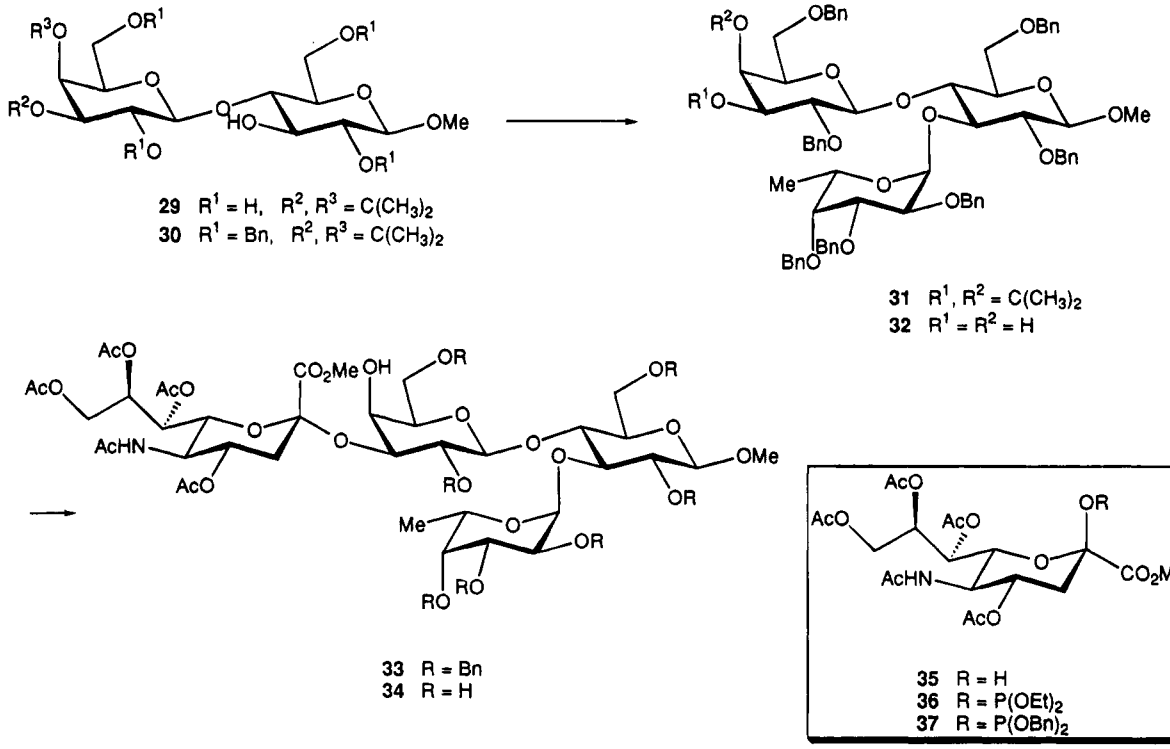

29 R^1 = H, $R^2, R^3 = C(CH_3)_2$
30 R^1 = Bn, $R^2, R^3 = C(CH_3)_2$

31 $R^1, R^2 = C(CH_3)_2$
32 $R^1 = R^2$ = H

33 R = Bn
34 R = H

35 R = H
36 R = P(OEt)$_2$
37 R = P(OBn)$_2$

the new glycosidic bond (δ 5.03, d, 1H, $J_{1',2'}$ = 3.7 Hz, H-1'). Deallylation of **25** using iridium catalyst[23] led to **26** having free the C-3' hydroxyl, which was glycosylated with 3,4,6-tri-*O*-acetyl-2-azido-2-deoxy-α-D-galactopyranosyl bromide[24] in the presence of mercuric bromide–mercuric cyanide to afford the protected tetrasaccharide **27** accompanied by traces of an impurity which could not be removed. Acetolysis of the 1,6-anhydro bond of **27** was tried with sulfuric, triflic, and acetic acids, in the presence of acetic anhydride in different ratios, leading in all cases to a large proportion of cleavage of the fucosyl residue. On the basis of the armed/disarmed concept in the reactivity of glycosidic bonds,[25] we envisaged that the exchange of benzyl groups in **27** with acetyl groups would increase the stability of the fucosyl linkage. Thus, catalytic hydrogenolysis (Pd–C) of **27** followed by acetylation gave the acetylated tetrasaccharide **28**. Acetolysis of **28** furnished a compound unseparable from the starting material, and the ^{1}H-NMR analysis of the mixture revealed the fucosyl residue intact. This mixture was directly treated with NaOMe to give, after column chromatography, the target tetrasaccharide **2** (64%). Alternatively, *O*-deacetylation of **28** led to **5**.

The synthesis of **3** was carried out in six steps starting from methyl 3',4'-*O*-isopropylidene-β-lactoside[26] (**29**, Scheme 5). Partial benzylation[27] of **29** gave as main product the expected tetrabenzyl derivative **30** having free the less reactive hydroxyl at C-3 (30%). α-L-Fucosylation under similar conditions as described above gave the protected trisaccharide **31** (82%, δ 5.63, $J_{1',2'}$ = 4.0 Hz, H-1'), which was treated with 80% acetic acid to afford diol **32**.

(23) Oltvoort, J. J.; van Boeckel, C. A. A.; de Konong, J. H.; van Boom, J. H. *Synthesis* **1981**, 305.
(24) Lemieux, R. U.; Ratcliffe, R. M. *Can J. Chem.* **1979**, *57*, 1244.
(25) Mootoo, D. R.; Konradsson, P.; Udodong, U.; Frase-Reid, B. *J. Am. Chem. Soc.* **1988**, *110*, 5583. Konradsson, P.; Mootoo, D. R.; McDevitt, R. E.; Fraser-Reid, B. *J. Chem. Soc., Chem. Commun.* **1990**, 270. Fraser-Reid, B.; Wu, Z.; Udodong, U. E.; Ottosson, H. *J. Org. Chem.* **1990**, *55*, 6068.
(26) Dahmen, J.; Gnosspelius, G.; Larsson, A.-C.; Lave, T.; Noor, G.; Palsson, K.; Frejd, T.; Magnusson, G. *Carbohydr. Res.* **1985**, *138*, 17.
(27) Fernández-Mayoralas, A.; Martín-Lomas, M.; Villanueva, D. *Carbohydr. Res.* **1985**, *140*, 81.

Chart 1

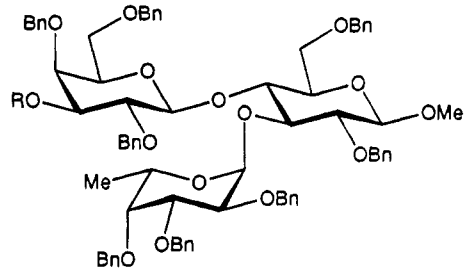

38 R = H
39 R = SO_3H

The sialylation on **32** was performed with the phosphite donor **36**,[28a] easily prepared from **35**. The reaction using trimethylsilyl triflate as catalyst at −40 °C for 1 h gave regio- and stereospecifically the tetrasaccharide derivative **33** in 36% yield (80% based upon **32** consumed). The sialylation with donor **37**[29] under similar conditions gave a lower yield of **33** (20%) and a large amount of decomposed **37**. Hydrogenolysis of **33** led to **34** which after treatment with NaOMe afforded the targeted **3**. Probably, hydrolysis of the methyl ester occured during the workup after methanolysis.

Trisaccharide **4** was easily obtained from the known intermediate **38** (Chart 1), which is prepared in four steps from methyl β-lactoside using highly selective reactions.[30] Sulfation of **38** gave **39** which was converted to **4** by hydrogenolysis.

Conformational Analysis. The conformational study of **1**, **3**, and **5** using NMR, molecular mechanics, and *in vacuo* molecular dinamics (MD) has been carried out to obtain the accessible geometries of these oligosaccharides. Two different force fields and dielectric constants have been used, and models of single geometries and of ensemble average distributions have been chosen to calculate NOEs.

The study of the conformation of oligosaccharides related to Le^X is a topic of interest.[31] A number of studies in the last years have led to contradictory results.[32-38] Most of them have concluded that the fucosyllactosamine fragment is rigid, in agreement with the pioneer work of Lemieux's group.[39] Nevertheless, the geometry of the postulated conformer varies among them, and other authors have proposed equilibria.[40] The existence of equilibria is of prime importance in the recognition phenomenon since any bimolecular binding process is entropically unfavorable.[41] This rigid/flexible controversy is due to the lack of data to define the conformation of a carbohydrate in water.[42] The number of NOEs is small, and the problem of estimating torsion angles is not overdetermined, as it may be the case for proteins or nucleotides.[43] An additional shortcoming comes from the number of polar groups which makes molecular modeling[42] rather difficult, particularly in water. In addition, it has been experimentally shown that intermolecular hydrogen bonds, at least for small oligosaccharides,[44] do not play a role in defining the conformation in water, probably due to entropic reasons. Besides, the presence of the acetal group, and therefore, the anomeric effect,[45] poses a problem for devising a force field for sugars, although a number of them are now available. The simulation of oligosaccharides using molecular dynamics (MD) with water has started recently,[42,46] but the results are not conclusive with regard to the accuracy of the force field, probably due to the short time accessible with present-day computers. Some authors have included NOEs as energy terms in the force field. However, the scarcity of these may lead to a *virtual* conformation,[47] with no physical meaning. Since NMR parameters are averaged, no analysis can exclude the presence of minor conformers.

With respect to the GalNAc-Gal unit of **1** and **5**, the studies published[39,48] for analogues agree with flexibility, mainly around Ψ. For NeuNAc-Gal (of **3**), it has been proposed equilibria between several conformers, and only few reports based their data on just one. The conformations of Gal-1→4-Glc (**1** and **3**) and 3-*O*-fucosyllactose have also been studied with controversial conclusions. Gal-AnhGlc has been analyzed,[49] with a complicated solvent-dependent behavior.

Compound 1. Contour isoenergy plots obtained by CVFF[50] and AMBER[51] for the disaccharides of **1** are given in Figures 1 and 2. Although CVFF is not specifically

(28) (a) Martin, T. J.; Brescello, R.; Toepfer, A.; Schmidt, R. R. *Glycoconjugate J.* **1993**, *10*, 16. (b) Baggett, N.; Marsden, B. J. *Carbohydr. Res.* **1982**, *110*, 11.
(29) Kondo, H.; Ichikawa, Y.; Wong, C.-H. *J. Am. Chem. Soc.* **1992**, *114*, 8748.
(30) Santos-Benito, F. F.; Nieto-Sampedro, M.; Fernández-Mayoralas, A.; Martín-Lomas, M. *Carbohydr. Res.* **1992**, *230*, 185.
(31) Phillips, M. L.; Nudelman, E.; Gaeta, F. C. A.; Perez, M., Singhal, A. K.; Hakomori, S.-I.; Paulson, J. C. *Science* **1990**, *250*, 1130.
(32) (a) Lin, Y. C.; Hummel, C. W.; Huang, D. H.; Ichikawa, Y., Nicolaou, K. C.; Wong, C. H. *J. Am. Chem. Soc.* **1992**, *114*, 9283. (b) Ichikawa, Y.; Lin, Y. C.; Dumas, D. P.; Shen, G. J.; Garcia-Junceda, E.; Williams, M. A.; Bayer, R.; Ketcham, C.; Walker, L. E.; Paulson, J. C.; Wong, C. H. *J. Am. Chem. Soc.* **1992**, *114*, 9283.
(33) (a) Homans, S. W.; Forster, M. *Glycobiology* **1992**, 2, 143. (b) Rutherford, T. J., Spackman, D. G.; Simpson, P. J.; Homans, S. W. *Glycobiology* **1994**, *4*, 59.
(34) Wormald, M. R.; Edge, C. J.; Dwek, R. A. *Biochem. Biophys. Res. Commun.* **1991**, *180*, 1214.
(35) Mukhopadyay, C.; Miller, K. E.; Bush, C. A. *Biopolymers* **1994**, *34*, 21.
(36) Ball, G. E.; O'Neill, R. A.; Schultz, J. E.; Lowe, J. E.; Wetson, B. W.; Nagy, J. O.; Brown, E. G.; Hobbs, G. J.; Bednarski, M. D. *J. Am. Chem. Soc.* **1992**, *114*, 5449.
(37) Bergwerff, A. A.; van Kuik, J. A.; Schiphorst, W. E. C. M.; Koeleman, C. A. M.; van der Eijnden, D. H.; Kamerling, J. P.; Vliegenthart, J. F. G. *FEBS Lett.* **1993**, *334*, 133.
(38) Miller, K. E.; Mukhopadyay, C.; Cagas, P.; Bush, C. A. *Biochemistry* **1992**, *31*, 6703.
(39) (a) Lemieux, R. U.; Bock, K.; Delbaere, L. T. J.; Koto, S.; Rao, V. S. *Can. J. Chem.* **1980**, *58*, 631. (b) Thogersen, H.; Lemieux, R. U.; Bock, K.; Meyer, B. *Can. J. Chem.* **1982**, *60*, 44.
(40) (a) Ejchart, A.; Dabrowski, J.; von der Lieth, C.-W. *Magn. Reson. Chem.* **1992**, *30*, S105. (b) Ejchart, A.; Dabrowski. J. *Magn. Reson. Chem.* **1992**, *30*, S115.
(41) Searle, M. S.; Williams, D. H. *J. Am. Chem. Soc.* **1992**, *114*, 10690.
(42) French, A. D.; Brady, J. W. *Computer Modeling of Carbohydrate Molecules*; ACS Symposium Series 430; American Chemical Society: Washington D.C., 1990.
(43) (a) Wüthrich, K. *NMR of Proteins and Nucleic Acids*; Wiley: New York, 1986. (b) Wüthrich, K. *Acc. Chem. Res.* **1989**, *22*, 36.
(44) (a) Leeflang, B. R.; Vliegenthart, J. F. G.; Kroon-Batenburg, L. M. J.; van Eijck, B. P.; Kroon, J. *Carbohydr. Res.* **1992**, *230*, 41. (b) Adams, B.; Lerner, L. *J. Am. Chem. Soc.* **1992**, *114*, 4827.
(45) (a) Lemieux, R. U.; Chu, N. J. *Abstracts of Papers*, 133rd National Meeting of the ACS, 1958, *31N*, San Francisco. (b) Tvaroska, I.; Bleha, T. *Adv. Carbohydr. Chem. Biochem.* **1989**, *47*, 45.
(46) (a) Brady, J. W.; Schmidt, R. K. *J. Phys. Chem.* **1993**, *97*, 958. (b) van Eijck, B. P.; Hooft, R. W. W.; Kroon, J. *J. Phys. Chem.* **1993**, *97*, 12093.
(47) (a) Cumming, D.; Carver, J. P. *Biochemistry* **1987**, *26*, 6664. (b) Carver, J. P. *Pure Appl. Chem.* **1993**, *65*, 763.
(48) (a) Stortz, C. A.; Cerezo, A. S. *J. Carbohydr. Chem.* **1994**, *13*, 235.(b) Bock, K.; Brignole, A.; Sigurskjold, B. W. *J. Chem. Soc., Perkin Trans. 2* **1986**, 1711. (c) Poppe, L.; Dabrowski, J.; von der Lieth, C.-W.; Koike, K.; Ogawa, T. *Eur. J. Biochem.* **1990**, *189*, 313.
(49) Rivera-Sagredo, A.; Jiménez-Barbero, J. *Carbohydr. Res.* **1991**, *215*, 239.
(50) (a) Hagler, A. T.; Huler, E.; Lifson, S. *J. Am. Chem. Soc.* **1974**, *96*, 5319. (b) Hagler, A. T.; Lifson, S.; Dauber, P. *J. Am. Chem. Soc.* **1979**, *101*, 5122.
(51) Weiner, S. J.; Kollman, P. A.; Case, D. A.; Singh, U. C.; Ghio, C.; Alagona, G.; Profeta, S., Jr.; Weiner, P. *J. Am. Chem. Soc.* **1984**, *106*, 765.

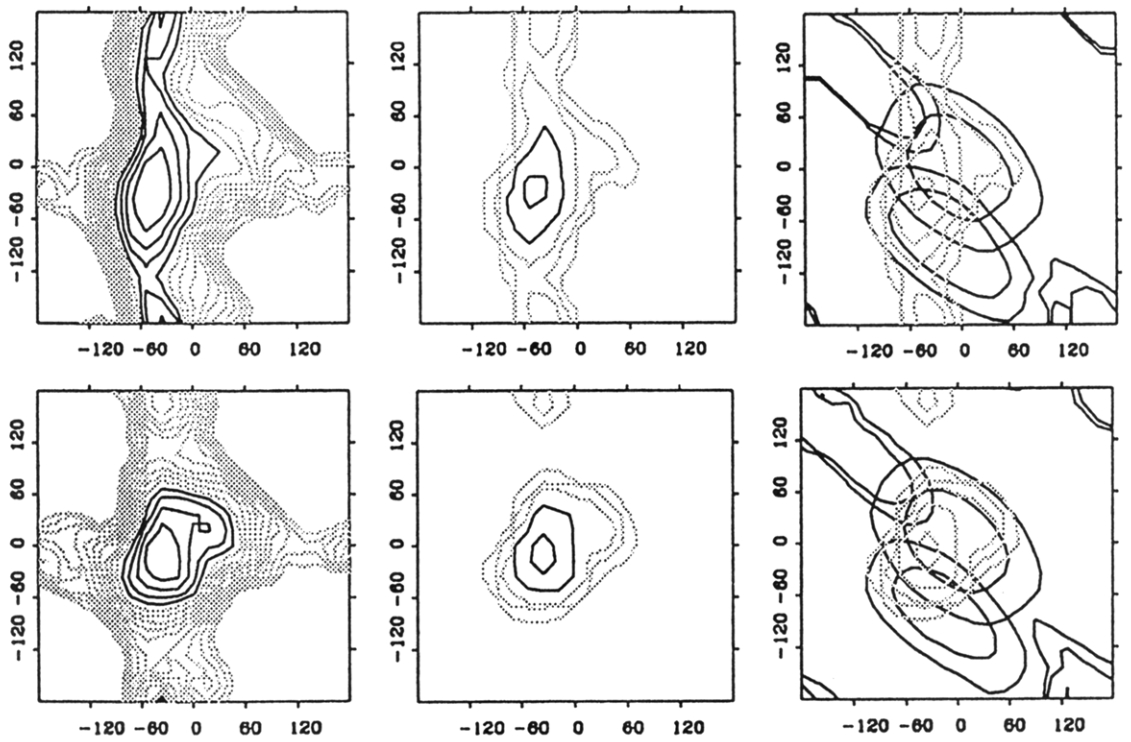

Figure 1. Relaxed steric energy maps (left) of the isoenergy contours (1 kcal/mol), populations (middle), and relevant interresidue proton distances (right), obtained by using AMBER (above) and CVFF (below) for the GalNAc-Gal fragment of **1** and **5**. Φ is indicated horizontally and Ψ along the vertical axis. Population contours are indicated at 10, 1, 0.1, 0.01, and 0.001%.

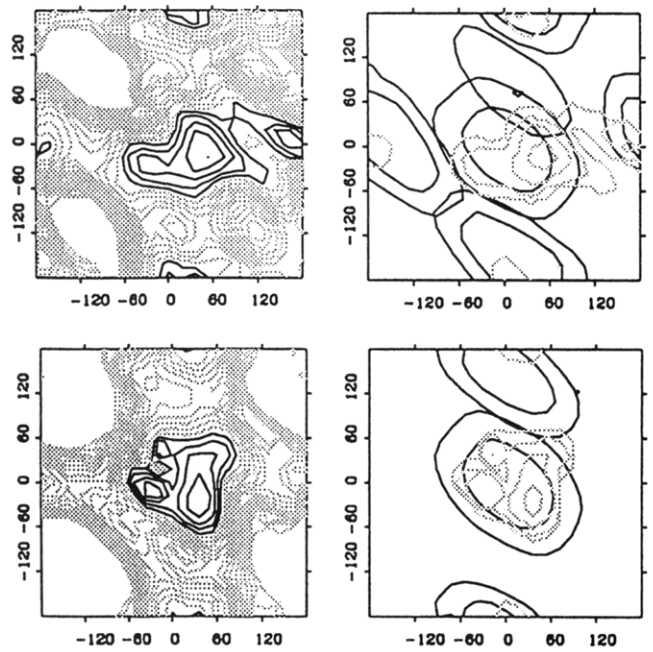

Figure 2. Relaxed steric energy maps (left) of the isoenergy contours (1 kcal/mol) and relevant interresidue proton distances superimposed on the population distributions (right), obtained by using CVFF for the Gal-Glc (top) and Fuc-Glc (bottom) isolated fragments of **1** and **3**. Φ is indicated horizontally and Ψ along the vertical axis. Population contours are indicated at 10, 1, 0.1, 0.01, and 0.001%.

parametrized for sugars, and therefore does not include any potential to account for the anomeric effect,[45] its use in conformational studies of oligosaccharides has produced satisfactory results.[52] AMBER has been modified[53] to deal with carbohydrates. There are several minima, with small energy barriers among them.[54] For Gal-Glc, *ca.* 8% of the surface is populated, while for GalNAc-Gal the low energy region occupies 10% of the map (AMBER). Finally, Fuc-Glc has fluctuations around 6% of the surface. Conformers GalG1-GalG5 refer to lactose, while GGal1-GGal4 and FG1-FG3 belong to GalNAc-Gal and Fuc-Glc, respectively. Table 1 shows the energies and the inter-residue proton distances. These energies correspond to local minima and not to conformers having the exact Φ/Ψ value. The angles did not differ from those shown, independently of the force field/dielectric constant. Possible conformers of **1** were built from the low energy regions, and those with energy above 5 kcal/mol of the global minimum were neglected. The conformational entropies[47] are 1.6 (GalNAc-Gal, CVFF-AMBER), 1.5 (Gal-Glc, CVFF), and 1.0 (Fuc-Glc, CVFF-AMBER) kcal/mol.

There are significant changes in the torsions when passing from disaccharides to tetrasaccharide **1**: now GalG2 and GalG4 of Gal-Glc are not minima, and only GalG1 or GalG3 appear to be possible for **1**. The presence of GalG5 is reduced, since structures with this geometry are destabilized ($\Delta E > 4$ kcal/mol). Thus, the tendency of entities with equatorial β-(1→4) linkages to occupy the central low energy region of the map is enhanced when O-3 of Glc is substituted. When integrated in **1**, GGal1 splits into two minima, Φ values oscillate between −42 and −52°, and Ψ varies between −35 and −49° (GGal1A). Values of $\Phi = -35°$, $\Psi = -17$ to $-4°$ (GGal1B) are also observed (CVFF, $\epsilon = 1$). GGal2 and GGal3, with positive angles, are disfavored for both force fields, mainly at low dielectric constants. The Fuc-Glc angles are substan-

(52) Balaji, P. V.; Qasba, P. K.; Rao, V. S. R. *Biochemistry* **1993**, *32*, 12599.

(53) (a) Scarsdale, J. N.; Ram, P. Prestegard, J. H. *J. Comput. Chem.* **1988**, *9*, 133. (b) Homans, S. W. *Biochemistry* **1990**, *29*, 9110.

(54) (a) Rivera-Sagredo, A.; Solis, D.; Diaz-Mauriño, T. Jiménez-Barbero, J.; Martín-Lomas, M. *Eur. J. Biochem.* **1991**, *197*, 217. (b) Dowd, M. K., French, A. D., Reilly, P. J. *Carbohydr. Res.* **1992**, *223*, 15. (c) Fernandez, P. Jiménez-Barbero, J. *Carbohydr. Res.* **1993**, *248*, 15.

Table 1. Relevant Interatomic Distances (Å) and Steric Energy Differences (kcal/mol) for the Low Energy Conformers of the Isolated Disaccharide Moieties of 1

fragment	conformer (Φ/Ψ)				
Gal-Glc	GalG1	GalG2	GalG3	GalG4	GalG5
(Φ/Ψ)	50/4	30/−55	−30/−30	180/5	35/180
ΔE	0.0	0.4	0.5	1.8	1.7
$r_{1'4}$	2.3	2.3	2.2	>3.5	>3.5
$r_{1'3}$	>3.5	>3.5	>3.5	>3.5	1.8
$r_{1'6r}$	2.5	>3.5	>3.5	>3.5	>3.5
$r_{1'6s}$	2.5	>3.5	>3.5	>3.5	>3.5
GalNAc-Gal	GGal1	GGal2	GGal3		
(Φ/Ψ)	−38/−11	−38/167	27/13		
ΔE	0.0	5.0	1.8		
$r_{1''3'}$	2.4	3.7	2.3		
$r_{1''4'}$	2.9	4.2	4.1		
Fuc-Glc	FG1	FG2	FG3	FG4	
(Φ/Ψ)	38/−25	−28/−13	9/16	7/180	
ΔE	0.5	1.0	0.0	2.9	
$r_{1'''2}$	4.4	4.5	4.0	2.4	
$r_{1'''3}$	2.3	2.3	2.2	3.7	
$r_{5'''3}$	2.3	2.3	2.2	3.7	
NeuNAc-Gal	NG1	NG2	NG3		
(Φ/Ψ)	−36/−18	47/−5	171/−10		
ΔE	0.1	0.0	1.7		
$r_{3''ax3'}$	2.2	4.2	3.5		
$r_{3''eq3'}$	3.5	4.5	2.4		
$r_{3''ax4'}$	4.2	5.2	2.6		
$r_{3''eq4'}$	5.0	4.7	2.3		
$r_{8''3'}$	3.8	2.8	5.9		
$r_{8''4'}$	2.3	5.1	6.6		
Fuc-AnhGlcNAc	FA1	FA2	FA3	FA4	
(Φ/Ψ)	41/−18	−29/−38	53/25	15/42	
ΔE	0.0	1.9	3.1	3.3	
$r_{1'''2}$	3.5	4.9	2.3	2.2	
$r_{1'''3}$	2.2	2.4	2.7	2.4	
$r_{1'''4}$	3.6	2.4	4.5	4.3	
$r_{6'''4}$	3.3	>5	>5	>5	
Gal-AnhGlcNAc	GA1	GA2	GA3		
(Φ/Ψ)	64/−17	29/−69	54/23		
ΔE	0.0	1.9	3.1		
$r_{1'''2}$	3.5	4.9	2.3		
$r_{1'''3}$	2.2	2.4	2.7		
$r_{1'''4}$	3.6	2.4	4.5		
$r_{6'''4}$	3.3	>5	>5		

tially modified: FG1 disappears, FG2 remains (Φ = −45 ± 5°, Ψ = −15 ± 5°), and FG3 angles are much larger, the values depending on the force field and dielectric constant used: When CVFF is used (Figure 3), Φ/Ψ are *ca.* 40−50/20−30 . This minimum also appears when the regular AMBER is employed. In this case, a new minimum is detected, Φ 67 ± 3°, Ψ 56 ± 4°. When AMBER−Homans is used, and ϵ = 78 D, the position is shifted toward Φ/Ψ = 80/30°. In addition, for this force field, the accessible area is higher at ϵ = 78 than at 1 D. FG4 energy is too large to be considered. Therefore, the conformation of this linkage is rather complicated. Due to the interaction between Gal and Fuc, the relative contribution of dispersive and electrostatic forces may drive this linkage to one or other region, and different factors, such as the *exo*-anomeric effect, or the atomic charges are relevant for the global minimum geometry.

Next, the conformational stability of the conformers of **1** was studied by MD simulations with CVFF and AMBER. Different geometries were used at 300 or 400 °K. Some trajectories are displayed in Figure 4, and a summary of the results is shown in the supplementary material. No chair to chair or chair to boat interconversions were observed. The β-(1→4) linkage had average Φ/Ψ of 50 ± 10°/0 ± 10° (GalG1). The trajectories remained (>95%) in the low energy region. When the starting geometry was different (GalG5), the simulation resulted in a transition to this area in a few ps. With regard to Fuc-Glc, the simulations indicate that its

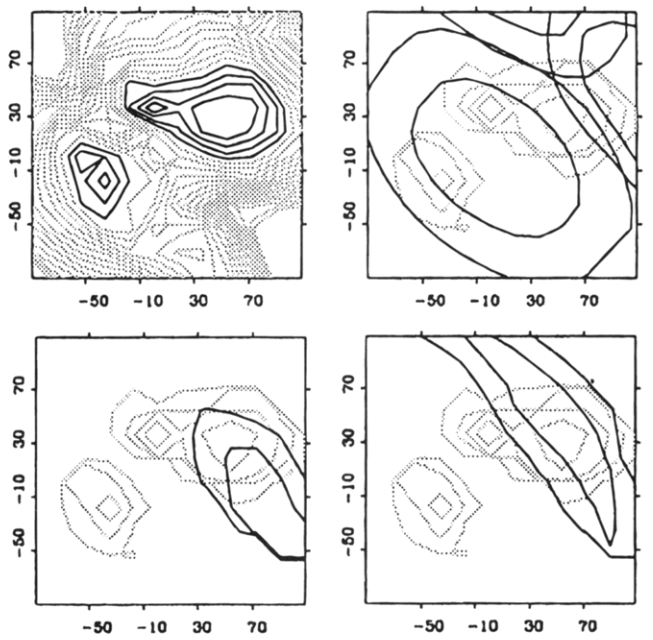

Figure 3. Relaxed steric energy map (left, top) of the isoenergy contours (2 kcal/mol) and relevant interresidue proton distances superimposed on the population distributions, obtained by using CVFF for the Fuc-Glc fragment when integrated in **1** or **3**. Φ is indicated horizontally and Ψ along the vertical axis. Population contours are indicated at 10, 1, 0.1, 0.01, and 0.001%.

flexibility is limited and there are motions smaller than 30° for Φ/Ψ (CVFF), mainly in FG3 region, with positive angles. Nevertheless, when AMBER is used and the initial geometry is FG2, the trajectory stays there. Finally, GalNAc-Gal shows a restriction around Φ (20°), independently of the force field, while Ψ oscillates 40°.

NMR spectroscopy can be used to distinguish the presence of either conformer.[55] The relevant distances for the interresidue protons are shown in Table 1 and Figures 1−3, superimposed on the energy maps of the disaccharides. When **1** as a whole is considered, there are also contacts between Gal and Fuc. When lactose is in GalG1 and Fuc-Glc in FG3A, Gal-H-2 is close to Fuc-H-5 and CH_3-6. On the other hand, for GalG3 of lactose, Fuc-H-5 is close to H-1 and H-5 of the β-Gal unit. Conformers FG2 and FG3B separate the Fuc and Gal rings. Interresidue NOEs and specific deshieldings impose constraints in the energy map to verify the presence of a given conformer.[55,56] The first step was to assign the signals of **1-5**, through COSY, TOCSY, and HMQC. The chemical shifts are shown in Tables 2−4. Fuc-H-1 is 0.3 ppm more deshielded in **1** than in the $SiLe^X$ analogue, **2**. Deshielding of Fuc-H-5 is observed in **1** and **2**. GalNAc H-5 is also deshielded. Since many factors influence chemical shifts, these facts may not be interpreted in terms of specific geometric relationships in a straightforward way, but indicate proximities of oxygens to Fuc-H-1, Fuc-H-5, and GalNAc H-5, which according to the calculated geometries may be due to Glc-O-2, Gal-O-5, and Gal-O-2, respectively.

Hydroxymethyl Conformation. The distribution of rotamers was calculated using well established method-

(55) (a) Homans, S. W. *Prog. NMR Spectrosc.* **1990**, *22*, 55. (b) Bush, C. A. *Curr. Opin. Struct. Biol.* **1992**, *2*, 655.

(56) Neuhaus, D.; Williamson, M. P. *The Nuclear Overhauser Effect in Structural and Conformational Analysis*; VCH Publishers: New York, 1989.

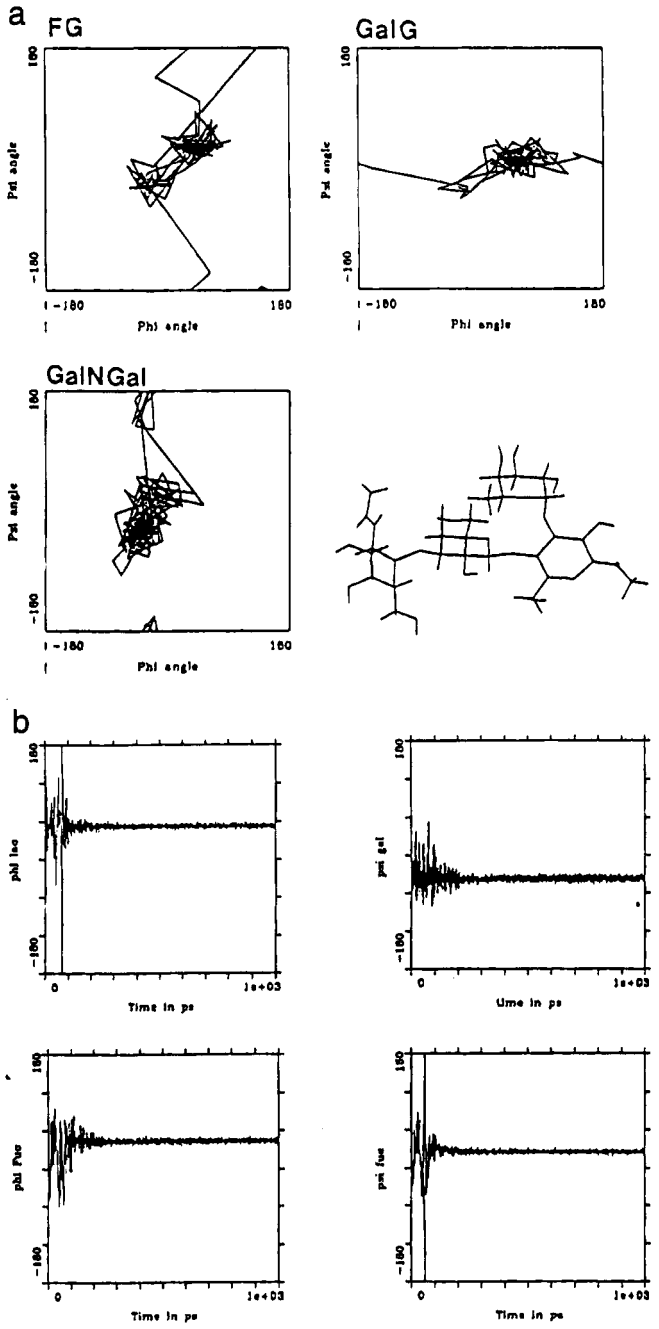

Figure 4. (a) Trajectory plots of one MD simulation of **1** using CVFF for 1 ns (ϵ = 78 D). FG: trajectory of the simulation in Φ/Ψ space for the Fuc-Glc fragment. GalG: lactose fragment. GalNGal: GalNAc-Gal fragment. The starting conformer for the simulation is also shown. (b) (Top, left) history of Φ angle of Gal-Glc. (Top, right) history of Ψ angle of GalNAc-Gal. (Bottom, left) history of Φ angle of Fuc-Glc. (Bottom, right) history of Ψ angle of Fuc-Glc.

ology.[57,58] The Glc couplings (2.1, 5.5 Hz) indicate a *ca.* 1:1 equilibrium between *gt:gg*. For GalNAc (6.4, 7.6 Hz) there is *ca.* 1:1 equilibrium between *gt:tg*. The couplings for β-Gal were not defined to determine its conformation. Similar behavior is found for **1** and **3**.

Analysis of NOE Data. There are different levels of interpreting experimental NOE data.[56] The initial rate or isolated spin-pair approximation (ISPA) may be used in experiments (NOESY, ROESY), acquired with short mixing times. The existence of NOE between Gal-H-1 and Glc-H-4, Gal-H-1-Glc-H-6 and neither between Gal-H-2 and Glc-H-4 nor Gal-H-1 and Glc-H-3 implies the presence of the GalG1 conformer. The corresponding average distances for Gal-H-1-Glc-H-4 and Gal-H-1-Glc-

(57) Nishida, Y.; Hori, H.; Ohrui, H.; Meguro, J. *J. Carbohydr. Chem.* **1988**, *7*, 239.
(58) Nishida, Y.; Ohrui, H. Meguro, H. *Tetrahedron Lett.* **1984**, *25*, 1575.

Table 2. ^{1}H and ^{13}C NMR Chemical Shifts (δ, ppm) for 1 in (A) D_2O and (B) DMSO-d_6 solutions at 37 °C

atom	solvent				solvent			
	^{1}H		^{13}C		Fuc			
Glc	A	B	A	B	A	B	A	B
H-1	4.38	4.10	105.5	102.8	5.46	5.15	100.5	98.8
H-2	3.51	3.22	76.7	74.0	3.81	3.46	70.3	68.6
H-3	3.79	3.46	79.0	78.8	3.97	3.63	71.5	69.2
H-4	3.88	3.58	75.3	64.2	3.78	3.46	74.3	71.8
H-5	3.54	3.25	76.9	75.3	4.77	4.59	68.5	66.0
H-6$_S$	4.00	3.76	61.9	59.4	1.21	1.00	18.3	16.5
H-6$_R$	3.84	3.68				4.14 (OH-3)		
OH-2		5.25				4.18 (OH-2)		
OH-6		4.64				4.04 (OH-4)		
Gal					GalNAc			
H-1	4.47	4.30	104.0	101.7	5.07	4.71	96.8	96.1
H-2	3.56	3.38	71.8	69.0	4.22	4.09	73.0	49.5
H-3	3.72	3.31	79.5	80.0	3.99	3.67	69.7	67.4
H-4	4.07	3.72	67.0	73.4	4.03	3.76	70.5	70.6
H-5	3.68	3.21	77.2	74.4	4.21	4.01	77.5	68.0
H-6$_R$	3.78	3.52	63.5	60.2	3.78	3.50	63.0	59.6
H-6$_S$	3.72	3.39			3.78	3.40		
OH-2		4.84				7.60 (NH)		
OH-4		3.98				4.03		
OH-6		4.44				4.45		
						4.46 (OH-3)		

Table 3. ^{1}H and ^{13}C NMR Chemical Shifts (δ, ppm) for 3 in D_2O Solution at 37 °C

	atom			
Glc	^{1}H	^{13}C	Fuc	
C-1	4.41	104.9	5.45	100.3
C-2	3.52	76.3	3.80	69.9
C-3	3.79	79.0	3.95	71.3
C-4	3.87	74.7	3.80	74.0
C-5	3.58	77.0	4.81	68.5
C-6	4.04/3.88	61.8	1.21	17.7
Gal			NeuNAc	
C-1	4.51	103.8		175.1
C-2	3.53	71.8		99.0
C-3	4.11	77.6	2.80/1.82	40.1
C-4	3.94	69.3	3.70	70.2
C-5	3.59	77.2	3.85	53.6
C-6	3.78/3.72	63.5	3.68	74.1
C-7			3.61	69.8
C-8			3.90	73.9
C-9			3.89/3.66	64.5

Table 4. ^{1}H and ^{13}C NMR Chemical Shifts (δ, ppm) for 5 in D_2O Solution at 37 °C

	proton atom			
1,6-AnhGlcNAc	^{1}H	^{13}C	Fuc	
C-1	5.51	102.9	5.04	103.1
C-2	3.90	52.5	3.80	70.1
C-3	3.97	78.2	3.84	71.8
C-4	3.94	79.3	3.82	74.8
C-5	4.83	75.3	4.11	68.7
C-6	4.20/3.82	67.6	1.23	17.9
Gal			GalNAc	
C-1	4.58	104.7	5.09	97.1
C-2	3.68	72.0	4.22	52.5
C-3	3.74	79.9	4.00	70.0
C-4	4.13	67.0	4.02	70.6
C-5	3.64	77.4	4.19	73.4
C-6	3.79	63.5	3.80	63.4

Table 5. Comparison between the Estimated Inter-Residue Distances (Å) from the Experimental NOESY (500 ms) and ROESY (300 ms) Intensities at 37 °C in D_2O Solutions and Those Obtained from MM Calculations ($\langle r^{-6}\rangle^{-1/6}$, Å) for Compounds 1, 3, and 5 at 37 °C in D_2O Solutions

cross peak	expl	calcd		cross peak	expl	calcd	
compd **1**				compd **3**			
Gal/Glc				Gal/Glc			
H-1′/4	2.2–2.3	2.5[a]	2.4[b]	H-1′/4	2.3–2.4	2.5[a]	2.4[b]
H-1′/6A	2.8–3.0	3.1	3.0	H-1′/6A	2.8–3.0	3.1	3.0
H-1′/6B	2.8–3.0	2.8	2.8	H-1′/6B	2.8–3.0	2.8	2.8
Fuc/Glc				Fuc/Glc			
H-1‴/2	3.0–3.2		3.4[c]	H-1‴/2	3.1–3.3		3.4[c]
H-1‴/3	2.6		2.4	H-1‴/3	2.5–2.6		2.4
H-5‴/3	>3.3		3.2	H-5‴/3	>3.3		3.2
Fuc/Gal				Fuc/Gal			
H-5‴/2′	2.6		2.5[c]	H-5‴/2′	2.6		2.5[c]
H-6‴/2′	2.7		3.2	H-6‴/2′	2.7		3.2
GalNAc/Gal				NeuNAc/Gal			
H-1″/3′	2.6–2.7	2.3[b]	2.5[a]	H-3ax/3′	2.6	2.9[b]	2.8[d]
H-1″/4′	2.4	2.8	2.4	H-3ax/4′	>3.1	4.5	4.0
				H-3eq/4′	>3.1	4.5	4.0
				H-8/3′	3.1	3.2	3.5
				H-8/4′	overlap	3.0	3.5
compd **5**							
Gal/AnhGlcNAc				Fuc/AnhGlcNAc			
H-1′/4	2.3–2.4	2.4[b]		H-1‴/2	2.6–2.8	3.3	3.1
H-1′/3	>3.2	3.5		H-1‴/3	2.3–2.4	2.2	2.3
H-1′/5	2.6–2.9	3.4		H-1‴/4	>3.3	3.4	3.3
GalNAc/Gal				H-6‴/4	>3.2	3.4	
H-1″/3′	2.6–2.7	2.3[b]	2.5[a]				
H-1″/4′	2.4	2.8	2.4				

[a] Ensemble average AMBER ($\epsilon = 78$). [b] Ensemble average CVFF ($\epsilon = 1$). [c] Average FG3 region only (CVFF). [d] Average among local minima NG1, NG2, NG3 (2:1:1, CVFF). The experimental values include those obtained for different NOESY and ROESY sets.

H-6 from MD simulations ($\langle r^{-6}\rangle$ average) are 2.3 and 2.9 Å. The results from the probability distributions are 2.4 and 3.0. The use of ISPA gave 2.3 and 2.8 Å (Table 5), for Gal-H-1-Glc-H-4, and Gal-H-1-Glc-H-6 distances, respectively, in agreement with MD. According to the calculations, Gal-H-1-Glc-H-3 and Gal-H-2-Glc-H-4 are larger than 3.2 Å, and in fact, their NOEs were not detected. All this data, at least semiquantitatively, indicate that the conformation of the lactose unit is well defined by GalG1. On the other hand, the NOEs for both Fuc-H-1-Glc-H-3 and Fuc-H-1-Glc-H-2 pairs cannot be explained by a unique conformer, and both FG3 conformations have to be invoked. ISPA gives distances of 2.6 and 3.0 Å, respectively, while in MD, Fuc-H-1-Glc-H-3 is 2.5 Å and Fuc-H-1-Glc-H-2 is higher than 3.2 Å. The long-range NOEs between Fuc and Gal also agree with FG3A, since Gal-H-2-Fuc-H-5 and Gal-Fuc-CH_3-6 peaks are observable. GalG3 can be discarded, since no Gal-H-1(or H-5)-Fuc-H-5 NOE is detected. Both FG3 conformers explain Fuc-H-1 deshielding, due to the vicinity of Glc-O-2. On the other hand, for FG3A, Fuc-H-5 is close to Gal-O-5. For GalNAc-Gal, the ISPA distances are 2.5 and 2.4 Å for GalNac-H-1-Gal-H-3 and GalNAc-H-1-Gal-H-4, respectively, in agreement with AMBER, while CVFF predicts a GalNac-H-1-Gal-H-4 distance larger than GalNac-H-1-Gal-H-3. The deshielding of GalNAc-H-5 is due to Gal-O-2.

A more rigorous method to evaluate the NOEs is to use the geometries of the minima to calculate the expected NOEs *via* a full relaxation matrix[59] using one conformer or an average[60,61] according to a Boltzmann function. These results are shown in the supplementary material. The correlation time (τ_c) was deduced by fitting the calculated and experimental NOEs for every intraresidue proton pair, basically fixed, and averaging among all of them. The τ_c for different rings were very similar. A qualitative indication of similar dynamical behavior of the three glycosidic linkages is deduced from T_1 ratios[62c] at 500/300 MHz. These ratios were the same (within 15%) for the anomeric protons. Similar tendency and ratio was found for **3** (including H-3 protons). For **1**, the comparison among the observed and calculated NOE intensities for the individual minima showed that a satisfactory match could be obtained by considering only conformer GalG1. This result is in agreement with the results of the calculations, which show an important destabilization of GalG2 and 3 of the lactose moiety of **1** when compared to the same conformers of the disaccharide. In conclusion, the results indicate that the flexibility around the $\beta(1\rightarrow4)$ linkage of **1** is limited, $\Phi = 60 \pm 10°$ and $\Psi = 0 \pm 10°$. Therefore, its conformational entropy is substantially reduced (to *ca.* 0.5 kcal/mol) when passing from the disaccaride to **1**. With regard to Fuc-Glc linkage, the results indicate that FG3A alone cannot quantitatively explain all the NOEs, since the observed Fuc-H-1-Glc-H-3 is smaller than that predicted, while the experimental Fuc-H-1-Glc-H-2 is higher than that estimated from this unique geometry. In addition, the predicted remote NOEs are overestimated (Gal-H-2-Fuc-H-5 (13%) and Gal-H-2-Fuc-CH3-6 (3%), while the experimental values are 5 and 2%, respectively). Although the time scale of motion around the linkages is not exactly known, these results indicate that moderate flexibility should be taken into account for the torsion angles, the tendency being toward higher torsion angles

(59) (a) Peters, T.; Brisson, J. R.; Bundle, D. R. *Can. J. Chem.* **1990**, *68*, 979. (b) Cagas, P.; Bush, C. A. *Biopolymers*, **1990**, *30*, 1123.

(60) Imberty, A.; Tran, V.; Perez, S. *J. Comput. Chem.* **1989**, *11*, 205.

(61) (a) Sabesan, S.; Duus, J. O.; Fukunaga, T.; Bock, K.; Ludvigsen, S. *J. Am. Chem. Soc.* **1991**, *113*, 3236. (b) Scarsdale, J. N.; Prestegard, J. H.; Yu, R. K. *Biochemistry* **1990**, *29*, 9843.

(62) (a) Siebert, H.-C.; Reuter, G.; Schauer, R.; von der Lieth, C.-W.; Dabrowski, J. *Biochemistry* **1992**, *31*, 6962. (b) Poppe, L.; Dabrowski, J. *Biochem. Biophys. Res. Commun.* **1989**, *159*, 618. (c) van Halbeek, H.; Poppe, L. *Magn. Res. Chem.* **1992**, 30, S74. (d) Acquotti, D.; Poppe, L. Dabrowski, J.; von der Lieth, C.-W.; Sonnino, S.; Tettamanti, G. *J. Am. Chem. Soc.* **1990**, *112*, 7772.

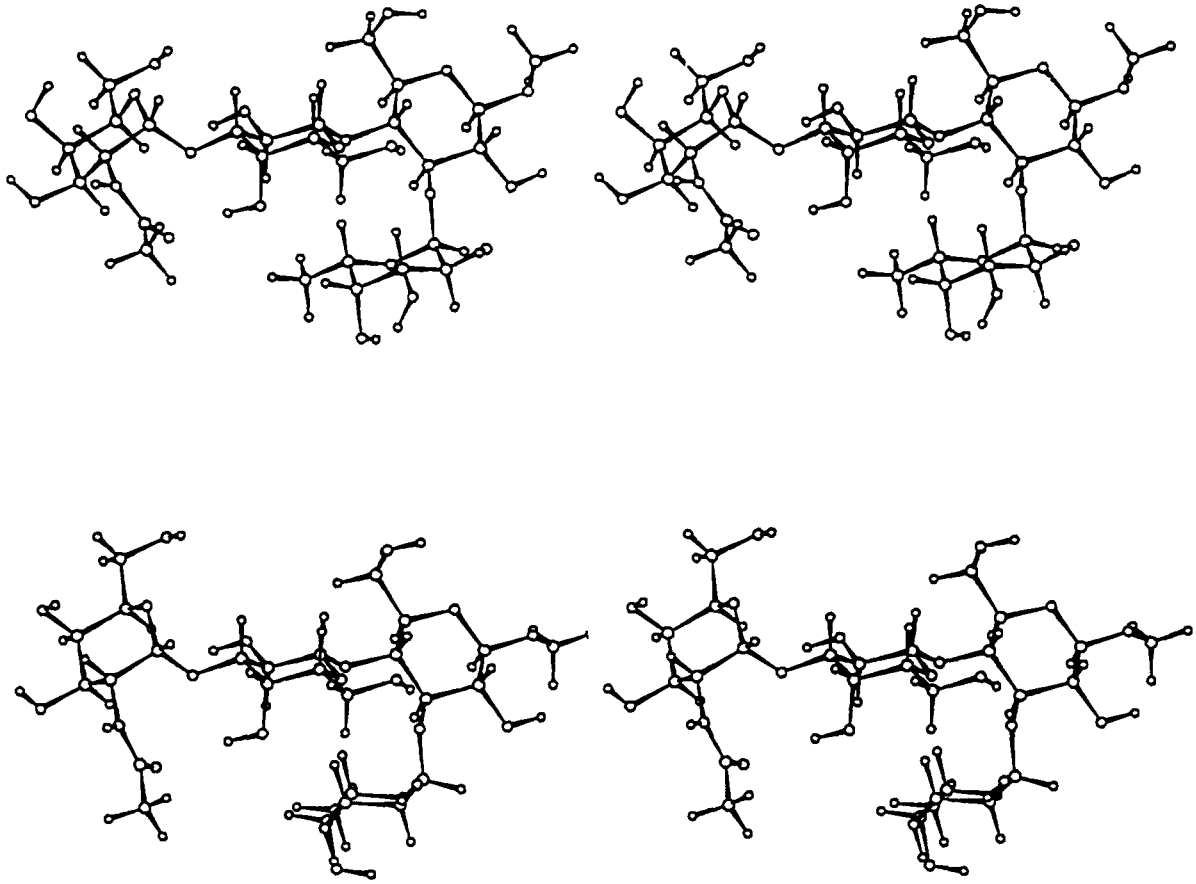

Figure 5. Stereoscopic view of the major conformers of **1** according to CVFF (top) and AMBER (bottom). Glycosidic torsion angles are indicated in the text.

(FG3B, Φ/Ψ, 70/60°). Since the region defined by both conformers has practically the same energy (ΔE < 2.0 kcal/mol), the mobility seems to be granted. This flexibility around the FG3 region (positive angles) may explain all observed and nonobserved NOEs, besides the deshieldings on Fuc-H-1 and Fuc-H-5, and therefore, the presence of population on FG2 region (negative values) may be discarded. According to the calculations and the experimental data, the conformational entropy for this linkage in the tetrasaccharide is reduced to 0.5 of that in the isolated disaccharide. With regard to GalNAc-Gal, the conclusion is similar, although both the presence of an unique conformer or the assumption of moderate flexibility around GGal1 quantitatively explains the experimental NOE and NOESY intensities. Nevertheless, we think, in accordance with the current opinion on oligosaccharide dynamics, that the second possibility is more feasible. Therefore, the conformational entropy associated to this moiety in **1** remains basically identical to that calculated for the free fragment. In conclusion, the recognition and freezing of the glycosidic linkages of **1** would cause an entropy loss of *ca.* 2.5 kcal/mol. The two major minima of **1** are depicted in Figure 5.

Since the conformation of $SiLe^X$ and analogues has been the subject of a number of reports on the past few years, we have compared our results with other previously reported results for analogues of **1** (Table 6). Most of these agree with the existence of a unique conformer. The conformers reported by Wong, Paulson, and coworkers,[32] based on GESA and MM2 calculations, qualitatively fit the NOEs, but fail to quantitatively explain the NOEs involving the Fuc moiety. A similar result is obtained for the conformers proposed by Lemieux's group[39] in which Gal-H-2/Fuc-H-5 and Gal-H-2/Fuc-H-6 NOEs are overestimated. The global minimum proposed by Homans and Forster and, recently, by Homans and co-workers,[33] based on restrained minimization, simu-

Table 6. Conformation of the Disaccharide Moieties of 1, 3, and 5 in Different Analogues

disaccharide	(Φ/Ψ)					ref
GalNAc/Gal						
	−30/50	−50/−40	−25/−175			40a
		−50/−34				40b
	−33/5	−31/−20				40c
	−36/−6	−55/−40				this work
Gal/Glc						
	60/5					29
	55/10					27
	50/0	50/15				32
			27/33			26
	55/30					25a
	49/13					25b
	55/5	46/12				24
	50/5					this work
Fuc/Glc						
	20/30	−40/−25	65/30			32
			55/30			27
	33/22					26
			43/26			25
	37/23		60/32	75/24		29
	24/30		48/24			24
	16/29	−45/−15	50/27	82/31	69/59	this work
NeuNAc/Gal						
	−35/−25	42/19	−166/34			54a
	−27/−26	35/12	−179/−14			54b
	−44/−30	35/10				54c
	−39/−18					54d
	−34/−13					53a
	−31/−22	58/3	21/−56			55a
			−160/50			53b
	−14−10	42/10				27
	−34/−20	44/−5	24/−57			25
	−44/−8	41/7	−172/−20	−77/−57		24
	−34/−20	45/−5	171/−10			this work

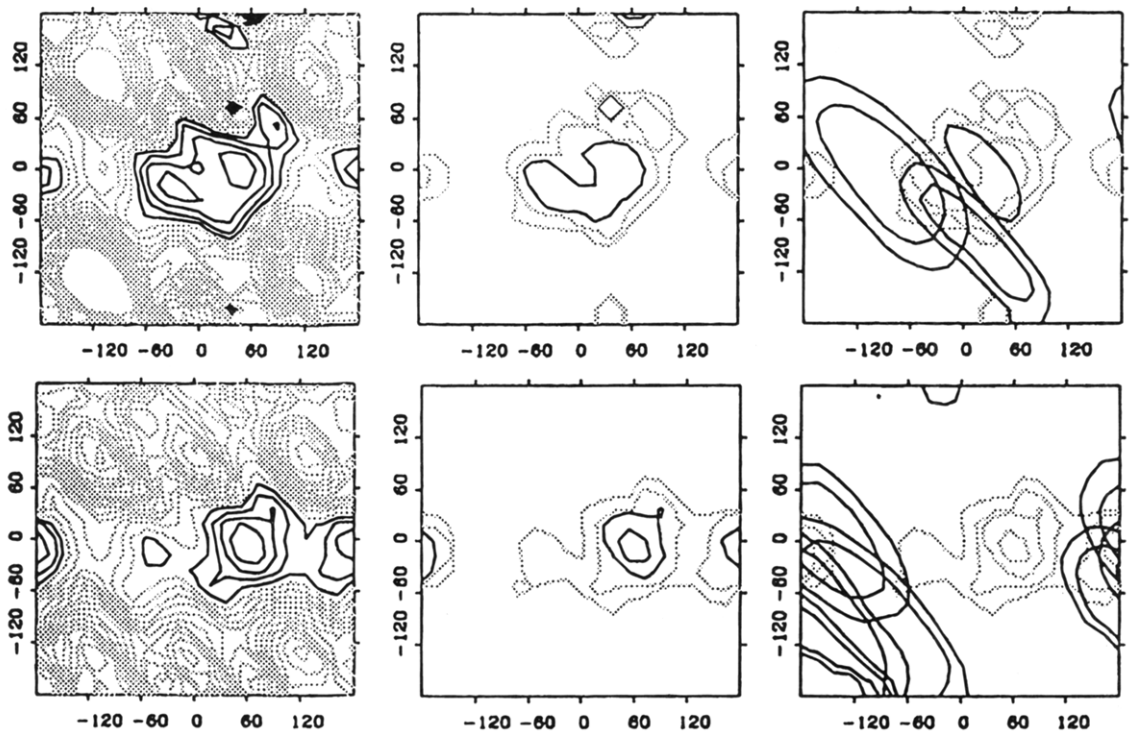

Figure 6. Relaxed steric energy maps (left) of the isoenergy contours (1 kcal/mol), populations (middle), and relevant interresidue proton distances (right), obtained by using CVFF (top) and AMBER (bottom) for the NeuNAc-Gal fragment of **3**. Φ is indicated horizontally and Ψ along the vertical axis. Population contours are indicated at 10, 1, 0.1, 0.01, and 0.001%.

lated annealing, and simulations, has the same characteristics and, in addition, underestimates Gal-H-1-Glc-H-4, overestimating the corresponding Gal-H-1-Glc-H-6 (high Ψ value, *ca.* 30°). However, the presence of moderate flexibility (10−20°) around the torsion angles is also considered. On the other hand, the minima of Dwek and co-workers,[34] based on AM1, show serious deviations from our NOEs. In this work the energy maps were calculated for the isolated disaccharide entities and, as explained above, the existence of interactions between remote moieties in the trisaccharide substantially modify the position of the minima. In contrast, the combination of the two sets of conformers proposed by Bush and co-workers[35,38] produces a satisfactory agreement with our data. These scattered results and the corresponding discrepancies are strongly related to the intrinsic nature of oligosaccharides which lack the sufficient number of distance constraints for a proper definition of the three-dimensional structure. In addition, the overlapping of key resonances, as is the case for GlcNAc-H2 in Le^X, poses an additional problem, which may lead to important ambiguities, which is not the case for **1**. Thus, Bednarski and co-workers[36] could detect the relevant GlcNAc-H-2/Fuc-H-1 in Le^X-β-*O*-allyl glycoside and suggested the existence of flexibility around the Fuc-Glc linkage, as we have shown. Finally, the conformation of mono- and difucosyl lactoses has been studied in DMSO by distance mapping, MM and MD calculations, and relaxation data.[40] The study presents two orientations for the fucoses, with lactose assuming a rigid conformation. While this conformer is basically the same proposed by us, they concluded the presence of both FG2 and FG3 conformers for Fuc-Glc.

Compound 3. The NOEs and chemical shifts for the 3-*O*-fucosyl lactoside are similar to **1**, and it can be assumed that its conformation remains the same and that there are no interactions among the sialic and the remote residues to cause changes around the Gal-Glc and Fuc-Glc linkages.

The conformation of NeuNAc-(2→3)-Gal has been previously studied with controversial results. The maps for the isolated disaccharide and the tetrasaccharide are similar. Six minima can be extracted from the relaxed energy maps. Both CVFF and AMBER (Figure 6) show an extended low energy area with three minima NG1, NG2, and NG3 with similar Ψ values (around 0 ± 20°), while Φ varies around 49−59 , −41 ± 10°, and 180°. According to AMBER, the energy barrier among these minima is *ca.* 3 kcal/mol, while CVFF estimates that the conformers with Φ *ca.* 55 and −40 are separated by 1 kcal and NG3 by 5 kcal/mol. In addition, three more minima NG4-NG6 are found with Φ 40−84° and Ψ being 55° (NG4, only CVFF) or close to 180° (NG5 and NG6). The conformational entropy is 2.5 kcal/mol, according to both AMBER and CVFF. AMBER MD simulations indicate that NG2 and NG3 are sampled during a 500 ps trajectory ($\epsilon = 78$), when the starting geometry is NG3. On the other hand, when the simulation is started with NG1, the trajectory remains there. Therefore, the conformational behavior of this linkage appears to be complicated, and the presence of mobility is deduced from the calculations. The superimpositions of the interresidue proton distances (Table 1) with the energy maps are also given in Figure 6. The orientation of the chain of the sialic acid was adjusted in that previously described.[35,61−63]

The NOEs indicate that there is major flexibility for NeuNAc-Gal since although the strongest NOE is Gal-H-3-NeuNAc H-3ax (NG1, NG3) weak Gal-H-4-NeuNAc H-3ax, Gal-H-3-NeuNAc H-8, and Gal-H-4-NeuNAc H-3eq NOEs are also observed. These are incompatible with a

(63) (a) Breg, J.; Kroon-Batenburg, L. M. J.; Strecker, G.; Montreuil, J.; Vliegenthart, J. F. G. *Eur. J. Biochem.* **1989,** *178*, 727. (b) Mukhopadhyay, C.; Bush, C. A. *Biopolymers* **1993**, *34*, 15.

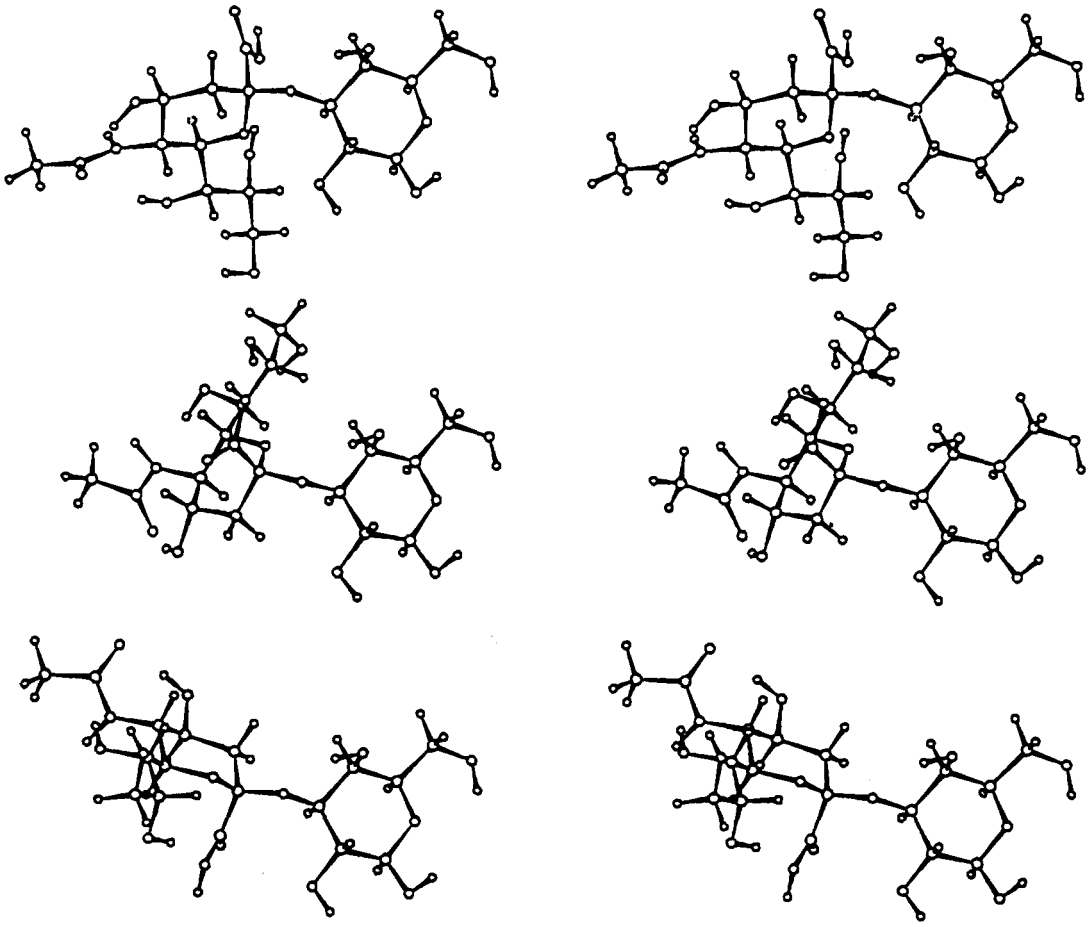

Figure 7. Stereoscopic view of the major conformers of the NeuNac-Gal fragment of **3**. NG2 (top), NG1 (middle), NG3 (bottom). Glycosidic torsion angles are indicated in the text.

single conformer, and according to the full matrix relaxation, even with moderate flexibility, there is a NG1:NG2:NG3 equilibrium, in 2:1:1 ratio.

Table 6 compares the angles of our minima with those proposed by other authors for compounds with the NeuNAc-Gal unit. NG1 and NG2 are present in most of the analysis, although some groups[61] have concluded NG1 alone. A study of GM4 ganglioside reported[62] on the presence of NG3. Breg *et al.* considered[63a] one additional conformer (25/−45) that, although it does not appear as a minimum in our maps, is included in the low energy region predicted by CVFF or AMBER. Other force fields agree with the presence of multiple conformers.[63b]

Therefore, the decrease of entropy upon binding of **3** to its receptor would amount to *ca.* 3.5 kcal/mol. Views of the low energy minima of **3**, and the superimposition of the ends of the major conformers of **1** and **3**, are given in Figures 7 and 8, respectively. There is no evident matching among the pyranoid rings.

Compound 5. Since the NMR parameters involving GalNAc are the same as described above for **1**, it can be concluded that its shape is basically the same as discussed above. The change in conformation of the Glc unit from $^4C_1$ to $^1C_4$ implies a major conformational variation on the remaining trisaccharide. Maps of Gal-AnhGlcNAc and Fuc-AnhGlcNAc using CVFF are included in the supplementary material. For the isolated Gal-AnhGlcNAc disaccharide, there are five local minima,[49] and three of them, GA1−GA3 (Φ/Ψ, 64/-17, 29/-69, 54/23), are located in an extended low energy region, with smaller energy values than the two islands. The conformational entropy is 2.7 kcal/mol. GA1−GA3 show short Gal-H-1-AnhGlcNAc-H-4 distances, while GA2 also presents short Gal-H-1-AnhGlcNAc-H-3, and GA3 has Gal-H-1-AnhGlcNAc-H-5 proximity. These geometries were used to build three minimized structures of **5**, which were employed for three relaxed maps in which Fuc-AnhGlcNAc angles were varied. GalNAc-Gal and Gal-AnhGlcNAc angles were let free during the minimization and remained at their starting positions with minor changes. The shape of these maps is similar since there is no coupling in the conformational behavior of both linkages. This is due to the diaxial orientation of AnhGlcNAc that locates the Gal and Fuc residues far away, and in addition, there is no possibility of inter-residue hydrogen bonding. The energies of the points in map GA1 are smaller than those in GA2 and GA3. Four minima are detected for Fuc-AnhGlcNAc, FA1 (41/-18), FA2(-30/-35), FA3 (53/24), and FA4 (16/42), whose distances are shown in Table 1. The conformational entropy (which is independent of Gal-AnhGlcNAc) is 1.5 kcal/mol.

The observed NOEs (supplementary material) indicate that there is flexibility for **5** since Gal-H-1 to AnhGlcNAc-H-4 and H-5 NOEs are measured, and that between Gal-H-1 and AnhGlcNAc-H-3 is detectable. The simultaneous presence of these NOEs implies conformational averaging within the low energy region, mainly close to GA1 and GA3. On the other hand, for Fuc-AnhGlcNAc, the existence of Fuc-H-1-AnhGlcNAc-H-3 and AnhGlcNAc-H-2 NOEs, and not between Fuc-H-1-AnhGlcNAc-H-4, indicates that this moiety is described by positive Φ angles, thus FA1, FA3, and FA4. The ISPA or relaxation matrix approaches (Table 5) also evidence that important flexibility of both linkages must be assumed to explain

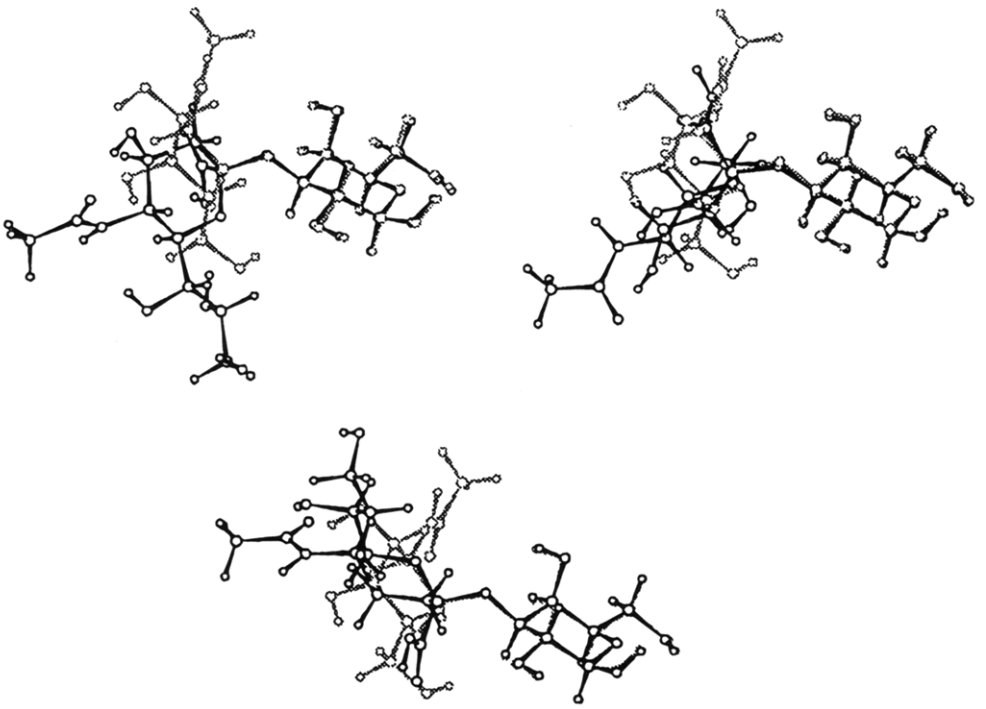

Figure 8. Superimposition of the major conformers of the terminal end of **3** with that of **1**.

the experimental results. Thus, the conformational entropy of **5** is *ca.* 5.5 kcal/mol, the most flexible compound of those studied herein. Figure 9 shows superimposition of the reducing ends of conformers of **1** and **5**, and it can be observed that the Fuc moiety has different orientations in both compounds.

As an overall conclusion, our results indicate that both force fields, in these conditions (*in vacuo*, bulk dielectric constant), do not quantitatively fit the NOEs and that only qualitative agreement is obtained. Geometries which agree with the exo-anomeric affect are found by both force fields, in spite of the fact that only AMBER (modified by Homans) contains parameters to deal with it. Therefore, although great improvement has been done in the prediction of carbohydrate crystals,[64] the theoretical modeling of the conformation of oligosaccharides in water can be misleading when experimental data (NOEs) are not available. Even with NOEs,[65] there are cases in which one cannot unambiguously deduce the presence of averaging or the existence of an unique conformer. Finally, although the found conformers are probably involved in the interaction with the natural receptor, van der Waals contacts or hydrogen bonding upon binding could change the saccharide geometries. Most of the protein–oligosaccharide complexes studied by X-ray or NMR agree with the binding of the major or one of the free ligand conformers, although there are exceptions.[66]

Biological Activity. The antimitotic activities of synthetic oligosaccharides were tested on both primary cultures of rat astrocytes and transformed cell lines, derived from astroglia (C6 glioma cells) and fibroblasts (3T3 cells). Oligosaccharides **1**–**4** inhibited tritiated thydimine incorporation promoted by 10% fetal serum, in all cell types (Table 7). However, antimitotic activity was higher on cells of neural origin (astrocytes and C6) than on those of fibroblastic origin (3T3). Tetrasaccharide **5** showed a dramatic loss of potency on astrocytes relative to compound **2**. Substitution of glucose in compound **1** for *N*-acetylglucosamine in compound **2** did

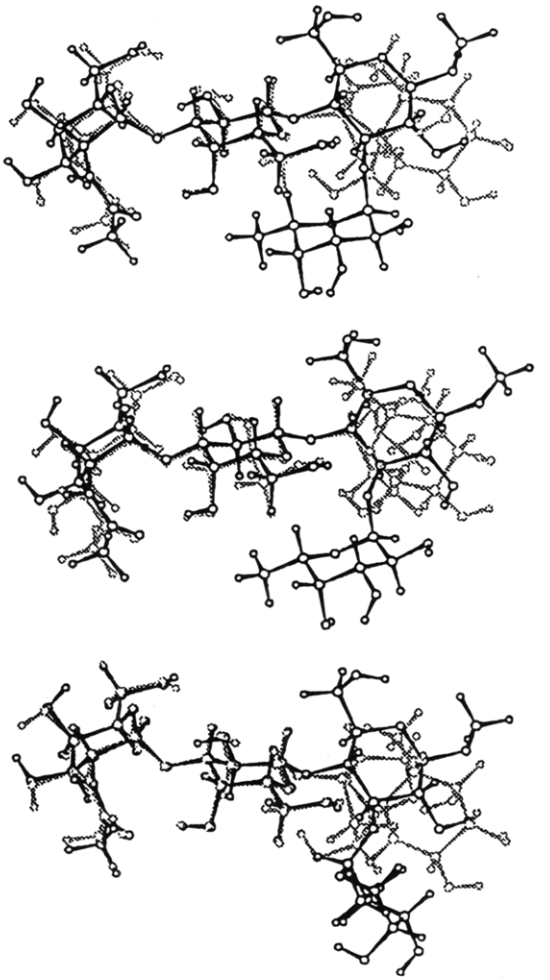

Figure 9. Superimposition of the major conformers of **5** with the major conformer of **1**.

(64) French, A. D.; Dowd, M. K. *J. Mol. Struct.* **1993**, *286*, 183.
(65) (a) Homans, S. W. *Glycobiology* **1993**, *3*, 551. (b) Rutherford, T. J., Partridge, J.; Weller, C. T.; Homans, S. W. *Biochemistry* **1993**, *32*, 12715.
(66) Imberty, A.; Bourne, Y.; Cambillau; C. Rouge; P. Perez, S. *Adv. Biophys. Chem.* **1993**, *3*, 71.

Table 7. Antimitotic Activity of Compounds 1–5

compd	ID_{50}[a] (μM)		
	astrocytes	C6	3T3
1	63	110	309
2	66	106	232
3	35	101	122
4	109	79	133
5	2300		

[a] ID_{50}, the oligosaccharide concentration that inhibited by 50% the incorporation of tritiated thymidine into the cells, promoted by 10% fetal calf serum, was measured as described previously.[5]

not appear to affect the antimitotic activity. However, substitution of *N*-acetylgalactosamine by neuraminic acid (compound **3**) resulted in a tetrasaccharide twice as active as compound **1**. Interestingly, a sulfate group in the 3″ position of 3-fucosyl-lactose gave a compound (**4**) much more active than the parent 3-fucosyl-lactose (ID_{50} = 4300 μM).[5] Compound **4** was somewhat less inhibitory than compound **1** on primary astrocytes, but more inhibitory than the tetrasaccharide on tumor forming C6 glioma cells. Accordingly, the antitumoral activity observed for compound **1** on transplanted rat glioma and neuroblastoma[6] could be more effective using compound **4**.

As it has been stated during the conformational analysis, there is not a fair correspondence with regard to the terminal GalNAc or NeuNAc moieties when **1** and **3** are superimposed. However, when considering the global minima for these compounds, it is true that there is an important arrangement of negative charge density throughout one of the faces of the oligosaccharides, due to the presence of an important number of hydroxyl groups from the fucose residue to the terminal end. This is also the case when the sulfate analogue is considered. When the fucose residue occupies a different orientation (as in **5**) the biological activity drastically reduces. Therefore, it could be the case that this distribution of charges and the orientation of the fucose moiety would be implicated in the recognition by the hypothetical natural receptor.

Experimental Section

Synthesis of Oligosaccharides. General Methods. Melting points are uncorrected. TLC was performed on silica gel GF_{254} with detection by charring with H_2SO_4. Column chromatography was performed on silica gel (230–400 mesh) or Bio-gel P-4. Chromatographic eluents are given as volume to volume ratios (v/v). Solvents were distilled over drying agents: dimethylformamide (DMF), CaO; dichloromethane (DCM), CaH_2; tetrahydrofurane (THF), sodium/benzophenone ketyl; and acetonitrile (MeCN), phosphorous pentoxide. ^{1}H-NMR spectra were measure at 500, 300, or 200 MHz. ^{13}C-NMR were obtained at 50 MHz.

***O*-(2,3,4,6-Tetra-*O*-benzoyl-β-D-galactopyranosyl)-(1→4)-1,6-anhydro-*endo*-2,3-*O*-(4-methoxybenzylidene)-β-D-mannopyranose (11).** A solution of trimethylsilyl triflate (0.2 M, 3.57 mL, 0.71 mmol) in DCM was added dropwise to a mixture of **7** (2 g, 7.17 mmol), 2,3,4,6-tetra-*O*-benzoyl-α/β-D-galactopyranosyl trichloroacetimidate (**10**) (5.83 g, 7.88 mmol), and 4 Å molecular sieves (ca. 1 g) in DCM (220 mL) at −20 °C under Ar, and the mixture was stirred for 2 h. Thereafter, the temperature of the stirred mixture was allowed to rise slowly from −20 °C to room temperature during 1 h. Triethylamine was added, and the mixture was stirred at room temperature for 15 min, filtered through Celite, and concentrated. The residue was purified by column chromatography (DCM–acetone, 50:1 → 40:1) to obtain **11** (4.20 g, 68%) as a syrup: $[\alpha]_D$ +48° (*c* 0.8, $CHCl_3$); ^{1}H NMR ($CDCl_3$) δ 8.12–6.88 (m, 24H), 6.00 (d, 1H, *J* = 3.4 Hz), 5.86 (dd, 1H, *J* = 10.4, 7.7 Hz), 5.63 (dd, 1H, *J* =10.4, 3.4 Hz), 5.55 (s, 1H), 5.42 (d, 1H, *J* = 3.1 Hz), 5.08 (d, 1H, *J* = 7.7 Hz), 4.65 (dd, 1H, *J* = 7.2 Hz), 4.52–4.44 (m, 3H), 4.37 (t, 1H, *J* = 7.2 Hz), 4.17 (dd, 1H, *J* = 6.9, 3.1 Hz), 4.13 (s, 1H), 3.92 (d, 1H, *J* = 7.0 Hz), 3.80 (s, 3H), 3.70 (t, 1H, *J* = 7.0 Hz). Anal. Calcd for $C_{48}H_{42}O_{15}$: C, 67.11; H, 4.93. Found: C, 66.63; H, 4.65.

***O*-(2,3,4,6-Tetra-*O*-benzoyl-β-D-galactopyranosyl)-(1→4)-1,6-anhydro-3-*O*-(4-methoxybenzyl)-β-D-mannopyranose (12).** A solution of trifluoroacetic acid (0.89 mL, 10.5 mmol) in DMF (6 mL) was added dropwise to a stirred mixture containing **11** (0.8 g, 0.93 mmol), sodium cyanoborohydride (1.6 g, 23.3 mmol), and 3 Å molecular sieves in DMF (8 mL) at 0 °C under Ar atmosphere. The mixture was stirred at room temperature for 24 h, filtered through Celite, and poured into ice-cold saturated $NaHCO_3$ solution. The aqueous phase was extracted with DCM, and the combined extracts were washed with saturated $NaHCO_3$ solution, dried (Na_2SO_4), and concentrated. Column chromatography of the residue (hexane–AcOEt, 2:1 → 1:1) gave **12** (0.53 g, 66%) as a syrup: $[\alpha]_D$ +33° (*c* 1, $CHCl_3$); ^{1}H NMR ($CDCl_3$) δ 8.10–6.86 (m, 24H), 5.97 (dd, 1H, *J* = 3.4, 0.9 Hz), 5.76 (dd, 1H, *J* = 10.4, 7.8 Hz), 5.52 (dd, 1H, *J* = 10.4, 3.4 Hz), 5.20 (br s, 1H), 4.76 (d, 1H, *J* = 7.8 Hz), 4.60 (dd, 1H, *J* = 11.4, 6.9 Hz), 4.48 (s, 2H), 4.46 (dd, 1H, *J* = 11.4, 5.6 Hz), 4.36 (d, 1H, *J* = 6.2 Hz), 4.29 (ddd, 1H, *J* = 6.9, 5.6, 0.9 Hz), 4.01 (d, 1H, *J* = 7.0 Hz), 3.94 (dd, 1H, *J* = 5.9, 1.3 Hz), 3.86 (br s, 1H), 3.80 (s, 3H), 3.63 (ddd, 1H, *J* = 11.7, 5.9, 2.3 Hz), 3.57 (dd, 1H, *J* = 7.0, 6.2 Hz), 2.87 (d, 1H, *J* = 11.7 Hz); ^{13}C NMR ($CDCl_3$) δ 166.05, 165.55, 165.50 and 165.08, 159.62, 133.69, 133.41, 133.32, 130.01, 129.75, 129.69, 129.59, 129.18, 128.85, 128.65, 128.55, 128.41, 128.29, 113.98, 101.80, 100.53, 76.82, 73.78, 73.07, 71.66, 71.49, 69.63, 68.00, 65.91, 64.48, 55.32. Anal. Calcd for $C_{48}H_{44}O_{15}$: C, 66.96; H, 5.15. Found: C, 66.82; H, 5.31.

***O*-(2,3,4,6-Tetra-*O*-benzoyl-β-D-galactopyranosyl)-(1→4)-1,6-anhydro-2-azido-2-deoxy-3-*O*-(4-methoxybenzyl)-β-D-glucopyranose (13).** A solution of triflic anhydride (203 μL, 1.21 mmol) in DCM (800 μL) was added to a stirred solution of pyridine (112.4 μL, 1.39 mmol) in DCM (2 mL) at −10 °C under Ar atmosphere. After 10 min, a solution of **12** (0.53 g, 0.61 mmol) in DCM was added. After being stirred for an additional 10 min at -10°C, the mixture was allowed to attain ambient temperature. After 1 h, the mixture was diluted with DCM, neutralized with $NaHCO_3$ solution (5%), washed with water, and dried (Na_2SO_4) and the solvent evaporated. The residue was dissolved in DMF (18 mL), and addition of NaN_3 (0.37 g, 5.61 mmol) was made at 0 °C. The reaction was stirred at room temperature for 18 h, and the solvent was evaporated under reduced pressure (bath temperature <30 °C). The residue was dissolved in DCM and washed with water, the aqueous phase was re-extracted with DCM, and the combined extracts were washed with water, dried (Na_2SO_4), and concentrated to give an oil which got crystallized. The crystals were washed with MeOH to give **13** (0.52 g, 96%): mp 175 °C; $[\alpha]_D$ +64° (*c* 0.9, $CHCl_3$); ^{1}H NMR ($CDCl_3$) δ 8.04–6.78 (m, 24H), 5.97 (dd, 1H, *J* = 3.4, 1.0 Hz), 5.83 (dd, 1H, *J* = 10.4, 7.9 Hz), 5.55 (dd, 1H, *J* = 10.4, 3.4 Hz), 5.36 (br s, 1H, *J* ≤ 1 Hz), 4.98 (d, 1H, *J* = 7.9 Hz), 4.57 (dd, 1H, *J* = 11.4, 6.6 Hz), 4.51 (m, 2H), 4.52–4.50 (m, 1H), 4.41 (dd, 1H, *J* = 11.4, 6.2 Hz), 4.26 (m, 1H), 3.95 (dd, 1H, *J* = 7.3, 1.4 Hz), 3.85 (m, 1H), 3.80 (m, 1H), 3.75 (s, 3H), 3.60 (dd, 1H, *J* = 7.3, 6.0 Hz), 3.19 (br s, 1H); ^{13}C NMR ($CDCl_3$) δ 165.99, 165.58, 165.50, 164.96, 159.48, 133.62–128.29, 113.92, 100.53, 74.09, 62.08, 59.58, 55.26. Anal. Calcd for $C_{48}H_{43}O_{14}N_3$: C, 65.06; H, 4.90; N, 4.75. Found: C, 64.99; H, 5.10; N, 4.83.

***O*-(3-*O*-Allyl-β-D-galactopyranosyl)-(1→4)-1,6-anhydro-2-azido-2-deoxy-3-*O*-(4-methoxybenzyl)-β-D-glucopyranose (15).** A solution of **13** (2.02 g, 2.29 mmol) in methanolic NaMeO (0.1 M, 15 mL) was stirred at room temperature for 15 h and then neutralized with Amberlite IR-120 (H^+), filtered, and concentrated. The residue was purified by column chromatography (AcOEt–methanol, 8:1 → 5:1) to give **14** (1.52 g, 84%) as a syrup: ^{1}H NMR ($CDCl_3$) δ 7.01 (AA′, 4H, Ar), 5.35 (s, 1H, H-1), 4.64 (d, 1H, H-1′), 4.51 (d, 2H, OCH_2Ar), 3.73 (s, 3H, OCH_3).

A mixture of **14** (0.126 g, 0.27 mmol), dibutyltin oxide (0.087 g, 0.345 mmol), and 3 Å molecular sieves in dry acetonitrile (6 mL) was stirred at 80 °C for 2 h. *N*-Methylimidazole (21.4

μL, 0.27 mmol) and allyl bromide (767 mL, 8.86 mmol) were added, and the reaction was stirred for 3.5 h. The mixture was filtered through Celite, the solid was washed with hot methanol, and the filtrate and washings were collected. A white solid which appeared in the filtrate was removed, and solvents were evaporated. Column chromatography of the residue (DCM–methanol, 30:1 → 20:1,) gave **15** (0.95 g, 70%): $[\alpha]_D$ +10° (*c* 0.6, $CHCl_3$). Anal. Calcd for $C_{23}H_{31}O_{10}N_3$: C, 54.22; H, 6.13; N, 8.25. Found: C, 53.95; H, 5.96; N, 7.98.

A sample of **15** was acetylated conventionally (pyridine/Ac_2O) to obtain **16**: ^1H NMR ($CDCl_3$) δ 6.99 (m, 4H) 5.77 (m, 1H), 5.58 (dd, 1H, *J* = 10.0, 8.0 Hz), 5.40 (dd, 1H, *J* = 3.4, 0.9 Hz), 5.35 (br s, 1H), 5.24 and 5.03 (2 m, 2H), 4.50 (d, 1H), 4.37 (dd, 1H, *J* = 6.0, 1.0 Hz), 4.15 (m, 2H), 4.22–4.18 (m, 2H), 4.10 (m, 2H), 3.82 (dd, 1H, *J* = 7.1, 1.0 Hz), 3.78 (m, 1H), 3.75 (m, 1H), 3.47 (m, 1H), 3.43 (m, 1H), 3.34 (dd, 1H, *J* = 10.0, 3.4 Hz), 3.32 (s, 3H), 3.05 (br s, 1H).

***O*-(3-*O*-Allyl-2,4,6-tri-*O*-benzyl-β-D-galactopyranosyl)-(1→4)-1,6-anhydro-2-azido-2-deoxy-3-*O*-(4-methoxybenzyl)-β-D-glucopyranose (17).** NaH (23.6 mg, 0.98 mmol) was added to a solution of **15** (81 mg, 0.16 mmol) in DMF (3.5 mL), and the mixture was stirred at room temperature for 45 min. Then benzyl bromide was added dropwise and stirring was continued for 12 h. Addition of MeOH and evaporation of the solvents rendered a residue that was purified by column chromatography (hexane → hexane–AcOEt, 3:1 → 2:1) to give **17** (92 mg, 74%) as a syrup: $[\alpha]_D$ +1° (*c* 1.1, $CHCl_3$); ^1H NMR (C_6D_6) δ 7.43–6.79 (m, 19H), 5.93 (m, 1H), 5.46 (br s, 1H), 5.32 and 5.17 (m, 2H), 4.60–4.58 (m, 1H), 4.43 (d, 1H, *J* = 7.7 Hz), 3.87 (m, 1H), 3.84 (m, 1H), 3.80 (dd, 1H, *J* = 7.9, 7.7 Hz), 3.76 (s, 3H), 3.75 (m, 1H), 3.68 (dd, 1H, *J* = 7.3, 6.0 Hz), 3.56–3.48 (m, 3H), 3.39 (dd, 1H, *J* = 7.9, 2.9 Hz) 4.38 (m, 2H), 4.20 (m, 1H), 3.97 (dd, 1H, *J* = 7.3, 0.9 Hz), 3.17 (br s, 1H). Anal. Calcd for $C_{44}H_{49}O_{10}N_3$: C, 67.76; H, 6.33; N, 5.39. Found: C, 67.48; H, 6.18; N, 5.10.

***O*-(3-*O*-Allyl-2,4,6-tri-*O*-benzyl-β-D-galactopyranosyl)-(1→4)-1,6-anhydro-2-azido-2-deoxy-β-D-glucopyranose (6).** To a stirred DCM (1.3 mL) solution of **17** (50 mg, 0.064 mmol) containing a small amount of H_2O (0.072 mL) was added 2,3-dichloro-5,6-dicyanobenzoquinone (34.8 mg, 0.076 mmol) at room temperature, and the mixture was stirred for 2.5 h. Solid was removed by decantation and washed with a small amount of DCM, and the combined DCM solutions were washed in sequence with saturated $NaHCO_3$ solution and water, dried (Na_2SO_4), and concentrated. Column chromatography (hexane–AcOEt, 3:1 → 1:1) of the residue gave **6** (33 mg, 78%) as a syrup which crystallized: mp 50–54 °C; $[\alpha]_D$ −40.4° (*c* 0.99, $CHCl_3$). Anal. Calcd for $C_{36}H_{41}N_3O_9$: C, 65.55; H, 6.26; N, 6.37. Found: C, 65.75; H, 6.51; N, 6.61.

A sample of **6** was acetylated conventionally (pyridine/Ac_2O): ^1H NMR ($CDCl_3$) δ 7.37–7.17 (m, 15H), 5.91–5.81 (m, 1H), 5.4 (s, 1H), 5.3–5.08 (m, 2H), 5.17 (t, 1H, *J* = 1.4 Hz), 4.44 (d, 1H, *J* = 7.6 Hz), 3.91 (d, 1H, *J* = 7.5 Hz), 3.82–3.76 (m, 2H), 3.66 (dd, 1H, *J* = 5.8, 7.5 Hz), 3.58 (s, 1H), 3.54–3.47 (m, 3H), 3.34 (dd, 1H, *J* = 9.7, 2.9 Hz), 3.12 (s, 1H), 1.94 (s, 3H).

***O*-(2,3,4,6-Tetra-*O*-benzoyl-β-D-galactopyranosyl)-(1→4)-1,6-anhydro-2,3-*O*-*endo*/*exo*-benzylidene-β-D-mannopyranose (20).** A solution of trimethylsilyl triflate (0.2 M, 2.44 mL) in DCM was added dropwise to a mixture of **19** (1.25 g, 5 mmol), the trichloroacetimidate **10** (3.7g, 5 mmol), and 4 Å molecular sieves (2 g) in DCM (125 mL) at −20 °C under Ar atmosphere, and the mixture was stirred for 2 h. Additional **10** (0.74g, 1 mmol) was added, and the temperature of the stirred solution was allowed to rise slowly from −20 to 0 °C during 2 h. Triethylamine (2 mL) was added, and the mixture was stirred at room temperature for 30 min, filtered through Celite, and concentrated. Column chromatography (DCM–acetone, 200:1) of the residue gave **20** (3.48g, 84%): mp 104–105 °C; $[\alpha]_D$ +51.7°(*c* 0.95, $CHCl_3$); ^1H NMR ($CDCl_3$) δ 8.06–7.16 (m, 25H), 5.93 (dd, 1H, *J* = 3.4, 0.9 Hz), 5.79 (dd, 1H, *J* = 7.8, 10.4 Hz), 5.55 (dd, 1H, *J* = 10.4, 3.4 Hz), 5.51 (s, 1H), 5.35 (d, 1H, *J* = 2.8 Hz), 5.01 (d, 1H, *J* = 7.8 Hz), 4.58 (dd, 1H, *J* = 7.2, 11.4 Hz), 4.45 (m, 3H), 4.30 (dd, 1H, *J* = 0.9, 7.2 Hz), 4.12 (dd, 1H, *J* = 3.1, 6.8 Hz) 4.07 (s, 1H), 3.85 (dd, 1H, *J* = 1.1, 7.4 Hz), 3.63 (dd, 1H, *J* = 6.3, 7.3 Hz). Anal. Calcd for $C_{47}H_{40}O_{14}$: C, 68.11; H, 4.86. Found: C, 67.99; H, 4.76.

***O*-(β-D-Galactopyranosyl)-(1→4)-1,6-anhydro-2,3-*O*-*endo*/*exo*-benzylidene-β-D-mannopyranose (21).** A solution of **20** (1.9 g, 2.29 mmol) in methanolic NaMeO (0.1M, 180 mL) was stirred at room temperature for 2 h and then neutralized with Amberlite IR-120 (H^+), filtered, and concentrated. The solid residue was washed with hexane (4 × 50 mL) and dried to obtain **21** (0.93g, 99%): $[\alpha]_D$ −68.2° (*c* 0.9, $CHCl_3$); ^1H NMR ($CDCl_3$) δ 7.7–7.37 (m, 5H), 6.26 (s, 1H), 5.77 (s, 1H), 5.51 (d, 1H, *J* = 2.8 Hz), 5.45 (d, 1H, *J* = 2.9 Hz), 4.53 (d, 1H, *J* = 7.3 Hz) 4.5 (d, 1H, *J* = 6.9 Hz), 4.38 (dd, 1H, *J* = 2.8, 6.0 Hz), 4.19 (dd, 1H, *J* =3 .0, 6.9 Hz), 4.11 (dd, 1H, *J* = 7.5, 1.2 Hz), 4.02 (dd, 1H, *J* = 7.5, 1.4 Hz). Anal. Calcd for $C_{19}H_{24}O_{10}$: C, 55.33; H, 6.04. Found: C, 55.01; H, 6.31.

***O*-(3-*O*-Allyl-β-D-galactopyranosyl)-(1→4)-1,6-anhydro-2,3-*O*-*endo*/*endo*-benzylidene-β-D-mannopyranose (22).** A mixture of **21** (0.606 g, 1.47 mmol), dibutyltin oxide (0.49 g, 1.91 mmol), *N*-methylimidazole (123 μL, 1.5 mmol), and 3 Å molecular sieves (1 g) in dry acetonitrile (33 mL) was stirred at 80 °C for 2 h. Allyl bromide (4.36 mL, 50.37 mmol) was added, and the reaction was stirred for 3 h at 80 °C. The mixture was cooled at room temperature and filtered through Celite, the bed was washed with methanol (4 × 30 mL), and the filtrate and washings were collected. A white solid appeared which was removed, solvents were evaporated, and the residue was chromatographed (DCM–MeOH, 10:1) to obtain **22** (0.43 g, 64%): $[\alpha]_D$ −55.4°(*c* 1.1, $CHCl_3$); ^1H NMR (CD_3OD) δ 7.67–7.33 (m, 5H), 6.22 (s, 1H), 6.05–5.95 (m, 2H), 5.72 (s, 1H), 5.45 (d, 1H), 5.41 (d, 1H), 5.37–5.15 (m, 4H), 4.51 (d, 1H, *J* = 6.7 Hz), 4.47 (d, 1H, *J* = 6.8 Hz), 4.35 (dd, 1H, *J* = 2.9, 6.1 Hz). Anal. Calcd for $C_{22}H_{28}O_{10}$: C, 58.4; H, 6.24. Found: C, 58.4; H, 6.38.

***O*-(3-*O*-Allyl-2,4,6-tri-*O*-benzyl-β-D-galactopyranosyl)-(1→4)-1,6-anhydro-β-D-mannopyranose (24).** Compound **22** (0.4 g, 0.885 mmol) was dissolved in DMF (35 mL), and NaH (0.26 g, 10.62 mmol) was carefully added. The mixture was stirred under Ar at room temperature for 1 h, and then dropwise addition of benzyl bromide (0.945 mL, 7.96 mmol) was made. The reaction mixture was stirred at room temperature for 2 h, cooled at 0 °C, and treated with MeOH (2 mL), added carefully. Solvents were evaporated, and the residue was extracted with DCM. Column chromatography (hexane–AcOEt, 4:1) of the residue gave **23** (0.53 g, 83%).

A solution of **23** (0.39 g, 0.54 mmol) in acetic acid (80%, 40 mL) was stirred at 75 °C for 2 h. The reaction mixture was concentrated, and column chromatography of the residue (hexane–AcOEt, 1:3) gave **24** (0.32 g, 92%) as a syrup: $[\alpha]_D$ −48.4° (*c* 1.2, $CHCl_3$); ^1H NMR ($CDCl_3$) δ 7.33–7.18 (m, 15H), 5.91–5.82 (m, 1H), 5.31 (s, 1H), 5.28–5.09 (m, 2H), 4.44 (d, 1H), 4.38 (d, 1H, *J* = 7.5 Hz), 4.15–4.08 (m, 2H), 4.02 (d, 1H, *J* = 7.3 Hz), 3.78 (s, 1H), 3.75 (d, 1H, *J* = 2.4 Hz), 3.7 (dd, 1H, *J* = 7.5, 9.7 Hz), 3.61 (dd, 1H, *J* = 5.8, 7.2 Hz), 3.33 (dd, 1H, *J* = 9.7, 3.0 Hz). Anal. Calcd for $C_{36}H_{42}O_{10}$: C, 68.12; H, 6.67. Found: C, 67.91; H, 7.01.

***O*-(3-*O*-Allyl-2,4,6-tri-*O*-benzyl-β-D-galactopyranosyl)-(1→4)-1,6-anhydro-2-azido-2-deoxy-β-D-glucopyranose (6).** To a solution of **24** (0.32 g, 0.50 mmol) and pyridine (406 mL, 5 mmol) in DCM (10 mL) under Ar at −40 °C was added triflic anhydride (126 mL, 0.75 mmol), and the reaction was stirred for 1.5 h at −40 °C until monotriflate was detected (TLC, hexane–AcOEt, 1:1) to be the major product (usually 1.5 h). The mixture was diluted with DCM (50 mL), neutralized with HCl (5%, 60 mL), washed with water (2 × 60 mL), and dried (Na_2SO_4), and the solvent was evaporated. The residue was dissolved in DMF (10 mL), and NaN_3 (0.32 g, 5 mmol) was added. The reaction was stirred at room temperature for 24 h. Water (60 mL) was added, and the crude was extracted with Et_2O. The ether extract was washed with water (3 × 60 mL) and dried (Na_2SO_4) and the solvent evaporated. Column chromatography (hexane–AcOEt, 1:1) gave **6** (0.25 g, 74%) as a syrup whose analytical and spectroscopic data agreed with the authentic sample obtained above following a different procedure.

***O*-(2,3,4-Tri-*O*-benzyl-α-L-fucopyranosyl)-(1→3)-[*O*-(3-*O*-allyl-2,4,6-tri-*O*-benzyl-β-D-galactopyranosyl)-(1→4)]-1,6-anhydro-2-azido-2-deoxy-β-D-glucopyranose (25).** A mixture of **6** (0.34 g, 0.516 mmol), $HgBr_2$ (0.062 g, 0.164 mmol), 4 Å molecular sieves (1 g), and DCM (10 mL) was stirred at

room temperature for 1 h. A solution of 2,3,4-tri-*O*-benzyl-α-L-fucopyranosyl bromide[22] (0.4 g, 0.79 mmol) in DCM (15 mL) was slowly added during 5 h, and the stirring was continued for 2 h. The mixture was filtered through Celite and the filtrate washed with NaI (10%) and saturated $NaHCO_3$ solution, dried (Na_2SO_4), and concentrated. Column chromatography of the residue (hexane–AcOEt, 4:1) gave **25** (0.38 g, 68%): $[\alpha]_D$ −46.5° (*c* 0.82, $CHCl_3$); ^1H NMR ($CDCl_3$) δ 7.37–7.11 (m, 30H), 5.89–5.83 (m, 1H), 5.42 (s, 1H), 5.29–5.09 (m, 2H), 5.03 (d, 1H, *J* = 3.6 Hz), 4.52 (d, 1H), 4.34 (d, 1H, *J* = 7.6 Hz), 4.16–4.12 (m, 2H), 4.01–3.98 (m, 1H), 3.95 (dd, 1H, *J* = 3.6, 10.1 Hz), 3.91–3.81 (m, 2H), 3.74 (dd, 1H, *J* = 10.0, 2.7 Hz), 3.71 (dd, 1H, *J* = 7.6, 9.7 Hz), 3.65 (d, 1H, *J* = 2.7 Hz), 3.60 (dd, 1H, *J* = 5.8, 7.2 Hz), 3.33 (dd, 1H, *J* = 9.7, 2.8 Hz), 3.2 (d, 1H), 0.98 (d, 3H, *J* = 6.4 Hz). Anal. Calcd for $C_{63}H_{69}N_3O_{13}$: C, 70.32; H, 6.42; N, 3.91. Found: C, 70.06; H, 6.7; N, 3.69.

***O*-(2,3,4-Tri-*O*-benzyl-α-L-fucopyranosyl)-(1→3)-[*O*-(2,4,6-tri-*O*-benzyl-β-D-galactopyranosyl)-(1→4)]-1,6-anhydro-2-azido-2-deoxy-β-D-glucopyranose (26).** A solution of **25** (0.24 g, 0.223 mmol) and $[Ir(COD)(PMePh_2)_2]$ PF_6 (2 mg) in THF (3 mL) was degassed and placed under H_2 atmosphere until the color of the solution turned from pale red to pale green. Then, H_2 was replaced by Ar and the reaction was stirred for 1 h at room temperature. Water (1 mL) and I_2 (0.06 g, 0.24 mmol) were added, and the mixture was stirred for 1 h. AcOEt (10 mL) was added, and the crude was washed with $Na_2S_2O_3$ (10%) and then with water, dried (Na_2SO_4), and concentrated. Column chromatography (hexane–AcOEt, 3:2) of the residue gave **26** (0.19 g, 80%): mp 140–141 °C; $[\alpha]_D$ −36° (*c* 0.78, $CHCl_3$); ^1H NMR ($CDCl_3$) δ 7.35–7.13 (m, 30H), 5.41 (s, 1H), 5.00 (d, 1H, *J* = 3.2 Hz), 3.99–3.86 (m, 3H), 3.75 (dd, 1H, *J* = 10.1, 2.8 Hz), 3.63 (dd, 1H, *J* = 2.5, 8.0 Hz), 1.01 (d, 3H, *J* = 6.8 Hz). Anal. Calcd for $C_{60}H_{65}N_3O_{13}$: C, 69.56; H, 6.28; N, 4.06. Found: C, 69.27; H, 6.28; N, 4.11.

***O*-(2,3,4-Tri-*O*-acetyl-α-L-fucopyranosyl)-(1→3)-[*O*-(2-acetamido-3,4,6-tri-*O*-acetyl-2-deoxy-α-D-galactopyranosyl)-(1→3)-*O*-(2,4,6-tri-*O*-acetyl-β-D-galactopyranosyl)-(1→4)]-2-acetamido-1,6-anhydro-2-deoxy-β-D-glucopyranose (28).** A mixture of **26** (0.145 g, 0.14 mmol), $Hg(CN)_2$ (0.177 g, 0.7 mmol), $HgBr_2$ (0.252 g, 0.7 mmol), 4 Å molecular sieves (1 g), and DCM (10 mL) was stirred for 1 h at room temperature and followed by addition of a solution of 3,4,6-tri-*O*-acetyl-2-azido-2-deoxy-α-D-galactopyranosyl bromide[24] (0.17 g, 0.43 mmol) in DCM (5 mL). After 24 h, additional $Hg(CN)_2$ (0.058 g, 0.23 mmol), $HgBr_2$ (0.092 g, 0.23 mmol), and glycosylating reagent (0.056 g, 0.14 mmol) were added and the reaction was stirred for 24 h. The mixture was filtered through Celite, washed with NaI (10%), saturated $NaHCO_3$ solution, and water, dried (Na_2SO_4), and concentrated. Column chromatography (hexane–acetone, 3:1) of the residue gave **27** accompanied by traces of an unseparable impurity: ^1H NMR ($CDCl_3$) δ 7.40–7.14 (m, 30H), 5.41 (s, 1H), 5.38 (dd, 1H, *J* = 11.0, 3.2 =Hz), 5,17 (d, 1H, *J* = 3.1 Hz), 5.02 (d, 1H, *J* = 3.7 Hz), 3.24 (d, 1H), 2.05, 2.01, 1.79 (3s, 9H), 1.00 (d, 3H, *J* = 6.4 Hz).

Compound **27** obtained as above dissolved in EtOH (10 mL) and Ac_2O (0.5 mL) was hydrogenolized in the presence of Pd/C (0.1 g) for 3 days at room temperature, filtered through Celite, and concentrated. The residue was treated with Ac_2O (2 mL) and pyridine (4 mL) for 8 h at room temperature and then concentrated. Column chromatography (DCM–acetone, 5:2) of the residue gave **28** (0.098 g, 64% from **26**): $[\alpha]_D$ −57.5° (*c* 0.99, $CHCl_3$); ^1H NMR ($CDCl_3$) δ 6.12 (d, 1H, *J* = 10.0 Hz), 6.05 (d, 1H, *J* =9.5 Hz), 5.38–5.33 (m, 3H), 5.22 (d, 1H, *J* = 3.8 Hz), 5.21 (dd, 1H, *J* = 9.2, 3.2 Hz), 5.03 (d, 1H, *J* = 3.5 Hz), 4.92 (dd, 1H, *J* = 9.2, 3.2 Hz), 4.62–4.52 (m, 1H), 4.44 (d, 1H, *J* = 7.0 Hz), 2.23, 2.13, 2.12, 2.11, 2.05, 2.03, 2.01, 2.00, 1.97, 1.96, 1.95, (11 s, 33H); 1.10 (d, 3H, *J* = 6.5 Hz). Anal. Calcd for $C_{46}H_{64}N_2O_{28}$: C, 50.55; H, 5.86; N, 2.56. Found: C, 50.31; H, 6.15; N, 2.62.

***O*-(α-L-Fucopyranosyl)-(1→3)-[*O*-(2-acetamido-2-deoxy-α-D-galactopyranosyl)-(1→3)-*O*-(β-D-galactopyranosyl)-(1→4)]-1,6-anhydro-2-acetamido-2-deoxy-β-D-glucopyranose (5).** A solution of **28** (35 mg, 0.032 mmol) in methanolic NaMeO(0.1M, 3.0 mL) was stirred at room temperature for 18 h and then neutralized with Amberlite IR-120 (H^+), filtered, and concentrated. The solid residue was washed with acetone (2 × 5 mL) and dried giving **5** (21 mg, 92%): $[\alpha]_D$ +4.3° (*c* 1.2, D_2O); ^1H and ^{13}C NMR, see Table 4. Anal. Calcd for $C_{28}H_{46}N_2O_{19}\cdot H_2O$: C, 45.90; H, 6.56; N, 3.82. Found: C, 45.52; H, 6.78; N, 3.71.

***O*-(α-L-Fucopyranosyl)-(1→3)-[*O*-(2-acetamido-2-deoxy-α-D-galactopyranosyl)-(1→3)-*O*-(β-D-galactopyranosyl)-(1→4)]-2-acetamido-2-deoxy-α,β-D-glucopyranose (2).** A mixture of **28** (35 mg, 0.032 mmol), trifluoroacetic acid/acetic acid (1/5, 1.2 mL), and sulfuric acid/acetic acid (1/10, 1.2 mL) was stirred at room temperature for 90 min. The reaction mixture was cooled at 0 °C, diluted with DCM (10 mL), and neutralized with saturated $NaHCO_3$ solution. The solvents were evaporated, and the reaction mixture was treated with methanolic NaMeO (0.1 M, 5 mL) for 2 h. The crude was neutralized with Amberlite IR-120 (H^+), filtered, and concentrated. Column chromatography (Bio-gel P-4) gave **2** (15 mg, 64% in two steps): $[\alpha]_D$ initial +39.4° $[\alpha]_D$ final +41.1° (*c* 0.88, D_2O); ^1H NMR (D_2O) δ 5.11 (d, 1H, *J* = 4.1 Hz), 5.06 (d, 1H, *J* = 3.8 Hz), 4.82–4.78 (m, 1H), 4.49 (d, 1H, *J* = 7.6 Hz), 4.47 (d, 1H, *J* = 6.7 Hz), 4.24 (dd, 1H, *J* = 3.7, 10.9 Hz), 3.70 (m, 1H), 3.66 (m, 1H), 3.56 (dd, 1H, *J* =7 .7, 9.8 Hz), 2.03, (s, 3H), 2.01 (s, 3H), 1.19 (d, 3H, *J* = 6.59 Hz). Anal. Calcd for $C_{28}H_{48}N_2O_{20}\cdot H_2O$: C, 44.80; H, 6.66; N, 3.73. Found: C, 44.63; H, 6.76; N, 3.71.

Methyl *O*-(2,6-Di-*O*-benzyl-3,4-*O*-isopropylidene-β-D-galactopyranosyl)-(1→4)-2,6-di-*O*-benzyl-β-D-glucopyranoside (30). A mixture of **29**[26] (1.0 g, 2.53 mmol), benzene (50 mL), sodium hydroxide (20%, 24 mL), and tetrabutylammoniumbisulfate (0.5 g, 1.47 mmol) was agitated vigorously at room temperature for 15 min. Benzyl bromide (2.0 mL, 16.81 mmol) was added dropwise during 24 h with stirring at room temperature. The reaction mixture was diluted with water, the organic phase separated, washed in sequence with water, sulphuric acid (1 M), and water (3 × 100 mL), dried (Na_2SO_4), and concentrated, and the residue chromatographed (hexane–AcOEt, 7:3) to obtain **30** (0.350 g, 20%) as a white solid: $[\alpha]_D$ +15° (*c* 0.9, $CHCl_3$);^1H NMR ($CDCl_3$) δ 7.23–7.41 (m, 20H), 3.58 (s, 3H), 3.3–4.9 (m, 15H), 1.60 (br, 1H, D_2O exchangeable), 1.39 (s, 3H), 1.32 (s, 3H); ^{13}C NMR ($CDCl_3$) δ 140.89, 140.88, 139.81, 139.58, 129.22–130.25, 112.01, 105.83, 104.64, 83.65, 83.43, 81.42, 81.22, 77.27, 76.58, 76.03, 75.55, 75.48, 75.27, 74.99, 74.10, 71.06, 70.59, 58.91, 29.64, 28.14. Anal. Calcd for $C_{44}H_{52}O_{11}$: C, 69.84; H, 6.87. Found: C, 70.04; H, 7.15.

Methyl *O*-(2,3,4-Tri-*O*-benzyl-α-L-fucopyranosyl)-(1→3)-[*O*-(2,6-di-*O*-benzyl-3,4-*O*-isopropylidine-β-D-galactopyranosyl)-(1→4)]-2,6-di-*O*-benzyl-β-D-glucopyranoside (31). A mixture of **30** (0.5 g, 0.66 mmol), $HgBr_2$ (0.120 g, 0.33 mmol), molecular sieves 4 Å (1.75 g), and 2,6-di-*tert*-butyl-4-methylpyridine (0.521 g, 2.54 mmol) in DCM (20 mL) was stirred under Ar for 1 h at room temperature. A solution of 2,4,6-tri-*O*-benzyl-α-L-fucopyranosyl bromide[22] (1.084 g, 2.18 mmol) in DCM (20 mL) was then added during 10 h, stirring was continued for 12 h, more $HgBr_2$ (0.023 g, 0.063 mmol) and 2,6-di-*tert*-butyl-4-methylpyridine (0.10 g, 0.487 mmol) were added, and the reaction was stirred for an additional period of 9 h. The reaction mixture was filtered through Celite, washed with aqueous NaI (10%), saturated $NaHCO_3$ solution, and water, dried (Na_2SO_4), and concentrated. Column chromatography (hexane–AcOEt, 10:1 → 5:1) of the residue gave **3** (0.635 g, 82%): $[\alpha]_D$ −26.0° (*c* 1.0, $CHCl_3$); ^1H NMR ($CDCl_3$) δ 7.02–7.25 (m, 35 H), 5.63 (d, 1H, *J* = 4.0 Hz), 4.31 (d, 1H, *J* = 8.0 Hz), 4.2 (d, 1H, *J* = 8.0 Hz), 3.40- 5.0 (m, 28H), 3.28 (m, 1H), 3.1 (dd, 1H), 1.27 (s, 3H), 1.21(s, 3H), 0.94 (d, 3H, *J* = 6.5 Hz); ^{13}C NMR ($CDCl_3$) δ 139.8, 139.6, 139.4, 139.0, 138.9, 138.8, 138.6, 130.0, 126.0, 110.0, 102.8, 101.0, 98.0, 83.6, 81.4, 80.3, 79.7, 78.4, 76.4, 76.2, 76.0, 75.8, 75.3, 75.1, 74.7, 74.2, 73.4, 73.3, 71.6, 71.2, 69.2, 68.3, 67.6, 66.0, 57.5, 29.0, 27.0, 17.5. Anal. Calcd for $C_{71}H_{81}O_{15}$: C, 72.69; H, 6.82. Found: C, 72.81; H, 6.62.

Methyl *O*-(2,3,4-Tri-*O*-benzyl-α-L-fucopyranosyl)-(1→3)-[*O*-(2,6-di-*O*-benzyl-β-D-galactopyranosyl)-(1→4)]-2,6-di-*O*-benzyl-β-D-glucopyranoside (32). A suspension of **31** (0.400 g, 0.34 mmol) in acetic acid:water (80:20, 200 mL) was stirred overnight at room temperature. The reaction mixture was concentrated and the residue chromatographed (hexane–

AcOEt, 7:3) to obtain **32** (0.290 g, 76%): $[\alpha]_D$ −20.5° (*c* 1.0, $CHCl_3$); ^1H NMR ($CDCl_3$) δ 6.8−7.65(m, 35 H), 5.63 (d, 1H, *J* = 4.0 Hz), 4.3 −5.0 (m, 23 H), 4.21 (d, 1H, *J* = 7.2 Hz), 3.6−4.15 (m, 7H), 3.49 (t, 1H, *J* = 9.5 Hz), 3.4 (s, 3H), 3.18−3.38 (m, 2H), 2.3 (br, 2H), 1.09 (d, 3H, *J* = 6.5 Hz); ^{13}C NMR ($CDCl_3$) δ 139.05, 138.95, 138.85, 138.03, 138.02, 138.01, 137.80, 128.57, 128.40, 128.27, 128.15, 128.02, 127.88, 127.71, 127.52, 127.44, 127.33, 127.26, 127.16, 127.03 126.91, 126.19, 124.33, 123.75, 123.18, 104.94, 101.97, 97.58, 79.95, 79.55, 78.35, 75.92, 75.75, 75.20, 75.07, 74.90, 73.60, 73.25, 73.10, 72.95, 72.75, 72.65, 72.20, 67.99, 65.70, 65.57, 56.93, 16.85. Anal. Calcd for $C_{68}H_{76}O_{15}$: C,72.08 ; H, 6.71. Found: C, 71.88 ; H, 6.91.

For compounds **35** and **37**, the literature procedures[28b,29] were followed.

Methyl *O*-(2,3,4-Tri-*O*-benzyl-α-L-fucopyranosyl)-(1→3)-[*O*-(methyl 5-acetamido-4,7,8,9-tetra-*O*-acetyl-3,5-dideoxy-D-*glycero*-α-D-*galacto*-2-nonulopyranosylonate)-(2→3)-*O*-(2,6-di-*O*-benzyl-β-D-galactopyranosyl)-(1→4)]-2,6-di-*O*-benzyl-β-D-glucopyranoside (33). A solution of the donor **37** (0.611 g, 1.0 mmol) and the acceptor **32** (1.698 g, 1.5 mmol), in dry acetonitrile (3.94 mL), was cooled to −40 °C. Under argon atmosphere, the catalyst TMSOTf (0.022 g, 0.1 mmol) dissolved in dry acetonitrile (0.5 mL) was added carefully. The reaction was stirred for (i) 15 min at −40 °C, (ii) 15 min at −37 °C, (iii) 30 min at −35 °C, and finally neutralized (pH 6.0−7.0) with triethylamine (0.018 mL) at the same temperature. The product mixture after evaporation under vaccum was chromatographed (toluene−acetone, 15:4 → 6:4) to obtain the unreacted acceptor **32** (1.0 g) followed by **33** (0.776 g, 36%) as a white solid: mp 82−85 °C; $[\alpha]_D$ −27.9° (*c* 0.55, $CHCl_3$); ^1H NMR ($CDCl_3$) δ 7.0−7.4 (m, 35 H), 5.2 (d, 1H, *J* = 4.0 Hz), 5.1 (d, 1H, NH), 4.52 (d, 1H, *J* = 8.0 Hz), 4.95−3.3 (m, 38H), 4.23 (d,1H, *J* = 8.0 Hz), 3.79 (s, 3H), 3.46 (s, 3H), 2.57 (br, 1H, D_2O exchangeable), 2.45 (dd, 1H, *J* = 4.7, 8.0 Hz), 2.10 (s, 3H), 2.02 (s, 3H), 1.96 (s, 3H), 1.90 (s, 3H), 1.88 (s, 3H), 1.18 (d, 3H, *J* = 7.0 Hz); ^{13}C NMR ($CDCl_3$) δ 170.71, 170.51, 170.27, 169.94, 168.34, 159.25, 139.34, 139.19, 138.81, 138.75, 138.62, 138.50, 138.31, 128.74, 128.35, 128.23, 128.18, 128.05, 127.93, 127.75, 127.63, 127.57, 127.50, 127.44, 127.37, 127.26, 127.09, 127.02, 126.92, 126.45, 104.96, 101.97, 98.85, 97.64, 83.14, 79.65, 78.79, 78.45, 76.32, 75.89, 75.45, 75.32, 75.22, 75.13, 73.45, 73.29, 73.15, 72.83, 72.55, 72.17, 69.15, 69.00, 68.20, 67.54, 67.32, 65.85, 62.28, 56.85, 53.02, 49.43, 36.12, 23.12, 21.05, 20.75, 20.70, 20.62, 20.48, 16.85. Anal. Calcd for $C_{88}H_{103}NO_{27}\cdot 4H_2O$: C, 62.96; H, 6.61; N, 0.83. Found: C, 62.76; H, 6.30; N, 1.03.

Methyl *O*-(α-L-Fucopyranosyl)-(1→3)-[*O*-(methyl 5-acetamido-4,7,8,9-tetra-*O*-acetyl-3,5-dideoxy-D-*glycero*-α-D-*galacto*-2-nonulopyranosylonate)-(2→3)-*O*-(β-D-galactopyranosyl)-(1→4)]-β-D-glucopyranoside (34). A solution of **33** (0.250 g, 0.155 mmol) in ethanol (18 mL) and ethyl acetate (2 mL) was treated with H_2 in the presence of 10% Pd−C (0.075 g) for 3 days at room temperature and then filtered through Celite and concentrated. Column chromatography (AcOEt−MeOH, 1:1) of the residue gave **34** (0.138 g, 92%) as a white solid: mp 179 °C; $[\alpha]_D$ −28.5° (*c* 0.4, CH_3OH); ^1H NMR (acetone-d_6) δ 6.80 (s, 1H), 5.49−5.30 (m, 3H), 5.35 (d, 1H, *J* = 4.0 Hz), 4.91(m, 1H), 4.9−3.3 (m, 18 H), 4.35 (m, 1H), 4.20 (d, 1H, *J* = 8.0 Hz), 4.10 (d, 1H, *J* = 8.0 Hz), 3.81 (s, 3H), 3.43 (s, 3H), 2.67 (dd, 1H, *J* = 4.7, 8.0 Hz), 2.08 (s, 3H), 2.06 (s, 3H), 1.98 (s, 3H), 1.94 (s, 3H), 1.77 (s, 3H), 1.18 (d, 3H, *J* = 6.5 Hz); ^{13}C NMR (acetone-d_6) δ 171.03, 170.73, 170.55, 170.52, 170.30, 169.45, 104.92, 103.56, 100.15, 99.35, 79.97, 78.23, 77.36, 76.12, 76.10, 75.97, 73.70, 73.25, 71.44, 70.74, 70.51, 70.14, 69.95, 69.02, 68.48, 66.94, 63.31, 62.38, 62.03, 56.77, 53.33, 49.82, 37.99, 23.01, 21.28, 20.88, 20.80, 20.77, 16.64. Anal. Calcd for $C_{39}H_{61}NO_{27}$: C, 48.0 ; H, 6.25 ; N, 1.43. Found: C, 47.82 ; H, 6.46 ; N, 1.33.

Methyl *O*-(α-L-Fucopyranosyl)-(1→3)-[*O*-(5-acetamido-3,5-dideoxy-D-*glycero*-α-D-*galacto*-α-nonulopyranosylonic acid)-(2→3)-*O*-(β-D-galactopyranosyl)-(1→4)]-β-D-glucopyranoside (3). A solution of **34** (0.116 g, 0.12 mmol) in methanol (100 mL) was treated with NaMeO (1.0 M, 1 mL) for 1 h at room temperature. The reaction mixture was cooled to 0 °C and neutralized with Dowex 50W-X8(H^+) resin to pH 4.0, filtered, and concentrated. The residue was lyophilized to obtain **3** as a white solid (0.074 g,78%): mp 240 °C; $[\alpha]_D$ −31.4° (*c* 0.5, H_2O); ^1H and ^{13}C NMR, see Table 3. Anal. Calcd for $C_{30}H_{51}NO_{23}\cdot 6H_2O$: C, 39.95; H, 6.99; N, 1.55. Found: C, 39.73; H, 6.65; N, 1.47.

Methyl *O*-[2,3,4-Tri-*O*-benzyl-α-L-fucopyranosyl-(1→3)-[*O*-(2,4,6-tri-*O*-benzyl-β-D-galactopyranosyl 3-sulfate)-(1→4)]-β-D-glucopyranoside (39). To a stirred solution of **38** (0.095 g, 0.077 mmol) in dry pyridine (5 mL) was added portionwise sulfur trioxide pyridine complex (0.247 g, 1.55 mmol). The mixture was stirred at room temperature until it was completed (13−15 h). Pyridine was removed under vaccum and the residue suspended in a H_2O/MeOH mixture. This suspension (pH acidic) was neutralized with KOH (0.5 M) and evaporated. The residue was extracted with methanol, evaporated, and chromatographed (AcOEt−methanol, 1:0 → 1:1) to obtain **39** (0.83 g, 82%): $[\alpha]_D$ −31° (*c* 0.5, MeOH); ^1H NMR (CD_3OD) δ 7.0−7.48 (m, 40H), 5.5 (d, 1H,*J* = 4.0 Hz), 3.30 (s, 3H), 1.13 (d, 3H, *J* =7.0 Hz); ^{13}C NMR (CD_3OD) δ 140.75, 140.50, 140.37, 140.18, 139.53, 139.45, 139.38, 130.25, 129.48, 129.37, 129.23, 129.18, 129.05, 128.88, 128.72, 128.66, 128.54, 128.32, 128.29, 128.09, 127.48, 105.99, 103.19, 98.71, 84.42, 82.32, 80.50, 80.46, 79.85, 79.43, 77.36, 76.91, 76.56, 76.33, 76.19, 74.62, 74.51, 74.20, 73.97, 73.86, 73.78, 73.33, 69.33, 69.05, 67.38, 55.20, 30.43. After several attempts satisfactory microanalysis for **39** could not be obtained.

Methyl *O*-(α-L-Fucopyranosyl(1→3)-[*O*-(β-D-galactopyranosyl 3-sulfate)-(1→4)]-β-D-glucopyranoside (4). A solution of **39** (0.080 g, 0.061 mmol) in EtOH was treated with Pd/C (10%) and H_2 gas until the disappearance (TLC) of **39** or any intermediate. The reaction was filtered over Celite and the Celite bed washed thoroughly with hot EtOH repeatedly. Solvent was evaporated, and the residue after silica gel chromatography (AcOEt−MeOH, 1:1) and lyophilization furnished **4** (0.033g, 92.2%): mp 240 °C dec; $[\alpha]_D$ −29° (*c* 0.4, H_2O); ^1H NMR (D_2O) δ 5.45 (d, 1H, *J* = 4.0 Hz), 4.78 (m, 1H), 4.54 (d, 1H, *J* = 8.0 Hz), 4.40 (d, 1H, *J* = 8.0 Hz), 4.32 (dd, 1H, *J* = 9.5, 2.5 Hz), 4.28 (dd, 1H, *J* = 2.5, <1.0 Hz), 3.57 (s, 3H), 1.19 (d, 3H, *J* = 7.0 Hz); ^{13}C NMR (D_2O) δ 104.43, 102.72, 99.61, 81.49, 78.20, 76.51, 75.91, 75.80, 74.13, 73.24, 70.52, 69.36, 67.97, 67.78, 62.61, 60.99, 58.54, 16.49. Anal. Calcd for $C_{19}H_{34}O_{18}S$: C, 39.17; H, 5.84; S, 5.49. Found: C, 38.82; H, 6.24; S, 5.84.

Conformational Analysis. Glucose (Glc) and *N*-Acetyl-1,6-anhydroglucosamine (GlcNAc) atoms are named unprimed, β-galactose (Gal) atoms are primed, *N*-Ac-galactosamine (NAc-Gal) and sialic atoms (NeuNAc) are double primed, and fucose (Fuc) atoms are triple primed.

NMR Experiments. NMR spectra were recorded at 37 °C in D_2O and DMSO-d_6, on Varian XL-300 and Unity 500 spectrometers. Proton chemical shifts were referenced to residual HDO at δ 4.61 ppm. Carbon chemical shifts to external dioxane at 67.4 ppm.

The double quantum filtered DQF-COSY experiments[67] were performed in the phase sensitive mode using the Varian sequence. The 2D-TOCSY experiments[68] were carried out using MLEV-17 for isotropic mixing. The 2D rotating frame NOE (ROESY, CAMELSPIN) experiments were recorded[69] with the rf carrier set at δ 5.5 ppm to minimize spurious Hartmann−Hahn effects.[69b,70] The 2D-NOESY experiments were carried out with mixing times of 500 and/or 700 ms for **1**, **3**, and **5**. The steady state 1D-NOE experiments were performed through the interleaved differential technique. The heteronuclear one bond proton−carbon correlation experiments were collected in the ^1H-detection mode using the HMQC[71] pulse sequence. The HSMQC-ROESY experiment[54c] was performed with the carrier set 100 Hz downfield from the

(67) Piantini, U.; Sorensen, O. W.; Ernst, R. R. *J. Am. Chem. Soc.* **1982**, *104*, 6800.

(68) Braunschweiler, R.; Ernst, R. R. *J. Magn. Reson.* **1983**, *53*, 521.

(69) (a) Bothner-By, A. A.; Stephens, R. L.; Lee, J.-M.; Warren, C. D.; Jeanloz, R. W. *J. Am. Chem. Soc.* **1984**, *106*, 811. (b) Bax, A.; Davis, D. G. *J. Magn. Reson.* **1985**, *63*, 207. (c) Bax, A. *J. Magn. Reson.* **1988**, *77*, 134.

(70) Leeflang, B. R.; Kroon-Batenburg, L. M. J. *J. Biomol. NMR* **1992**, *2*, 495.

(71) Bax, A.; Griffey, R. H.; Hawkins, B. L. *J. Magn. Reson.* **1983**, *55*, 301.

most deshielded resonance. NMR spin lattice relaxation times were determined through the inversion recovery technique using Varian software.

Molecular Mechanics and Dynamics Calculations. Glycosidic torsion angles are defined as Φ H-1−C-1−O-1−C-X, and Ψ C-1−O-1−C-X−H-X, except for NeuNAc in which Φ is defined as C-1−C-2−O-2−C-3. Relaxed (Φ,Ψ) potential energy maps were calculated for all the constituent disaccharides of compounds **1**, **3**, and **5** by using the AMBER and CVFF force fields. Only the *gg* (ω = 55°) and *gt* (ω = −175°) conformations of the lateral chains were used for the glucose and galactose residues, respectively, where ω is defined as O-6−C-6−C-5−C-4. The lateral chain of the sialic acid residue was considered to have a rigid orientation, according to previous results from different groups.[61-63] From the relaxed energy maps of the di- and tetrasaccharides, calculated for the different dielectric constants, the probability was calculated for each Φ/Ψ point of every linkage. Assuming that the entropy difference among the different conformers is negligible, the probability P of a given Φ/Ψ point is

$$P_{(\Phi\Psi)} = \exp(-E/RT)/\sum_{\Phi\Psi}[\exp(-E_{\Phi\Psi}/RT)]$$

The conformational entropy S associated with the ensemble was estimated[47] as

$$S = -R\sum(P_{(\Phi\Psi)} \ln P_{(\Phi\Psi)})$$

The estimated probability distributions were used to calculate average distances according to the well-known equations, valid for the ring protons:

$$\langle r^{-6}\rangle = \sum P_{(\Phi\Psi)} r^{-6}_{kl(\Phi\Psi)}$$

Molecular Dynamics. Different geometries describing local minima, obtained from the molecular mechanics protocole described above, all of them under a steric energy level of 5 kcal/mol from the global minimum, were extensively minimized (rms derivative < 0.001) and taken as starting structures for molecular dynamics simulations *in vacuo* by using AMBER and CVFF as integrated in Discover 2.9.[72] The trajectories were examined with the Analysis module of INSIGHT II.[73]

The steady state 1D-NOEs and NOESYs were calculated with the full relaxation matrix method using the NOEMOL program[74] for the coordinates of the local minima, for conformers included in regions centered in the local minima, for which Φ_H/Ψ_H differed up to 40° in 10° steps, and for geometries of reported conformers of Le^X. The presence of averaging was tested by calculating NOEs solving the set of linear equations of Noggle and Schrimer[75] and using the average relaxation rates obtained from the relaxed energies for each linkage. Isotropic motion and external relaxation of 0 or 0.1 s were assumed in the calculation. Different τ_cs were used in order to match the experimental and calculated NOE for a given intraresidue proton pair. Although the obtained τ_c for the different rings were basically the same (0.23−0.27 ns), this approach is a necessary oversimplification since both internal reorientation around glycosidic linkages[76] and librational motion of the C−H vectors within the ring[77] are taking place. NOESY and ROESY were used to estimate distances according to the isolated spin pair approximation. It was assumed that the cross relaxation rates are adequately represented by the cross peak volumes in these spectra.

Acknowledgment. Financial support by DGICYT (Grants PB 87-0367 and PB 90-0076), Comunidad de Madrid (Grants C258/91 and B0132/92), CICYT (Grant SAF 212/92), and Europharma S. A. are gratefully acknowledged. K.S. (on leave from the Department of Applied Chemistry, Guru Nanak Dev University, Amritsar, India) thanks the Ministerio de Educación y Ciencia for a postdoctoral fellowship.

Supplementary Material Available: Detailed experimental parts for the NMR experiments and the molecular mechanics and dynamics calculations. Figure 10 showing the history of the relevant interatomic distances for the MD simulation of **1**. Figure 11 showing the TOCSY spectrum of **3**. Figures showing 1D-NOEDIFF (Figure 12a) and HSMQC-ROESY (Figure 12b) spectra of **1**, 1D-NOEDIFF (Figure 13) and ROESY (Figure 14) spectra of **3**, and ROESY spectrum (Figure 16) of **5**. Figure 15 showing the relaxed steric energy maps and populations of the disaccharide fragments of **5**. Table VI with trajectories for MD runs of **1** and **3**, Tables VIIa, VIIIa, and IXa with experimental and calculated NOEDIFF intensities for **1**, **3**, and **5**, respectively, Tables VIIb, VIIIb, and IXb with experimental NOESY and ROESY and calculated NOESY intensities for **1**, **3**, and **5**, respectively, and Table X with T_1 ratio for different protons of **1** and **3** (20 pages). This material is contained in libraries on microfiche, immediately follows this article in the microfilm version of the journal and can be ordered from the ACS; see any current masthead page for ordering information.

JO9416877

(72) Discover 2.9 Program, Biosym. Technol., Inc., San Diego, CA.
(73) Insight II 2.1.0. Program, Biosym. Technol., Inc., San Diego, CA.
(74) Forster, M.; Jones, C.; Mulloy, B. *J. Mol. Graph.* **1989**, *7*, 196. QCPE Program 636, Chemistry Dept. Indiana Univ. Bloomington, IN, 1992.
(75) Noggle, J. H.; Schirmer, R. E. *The Nuclear Overhauser Effect: Chemical Applications*; Academic Press: New York, 1971.
(76) Hricovini, M.; Shah, R. N.; Carver, J. P. *Biochemistry* **1992**, *31*, 10018.
(77) Hajduk, P. J.; Horita, D. A.; Lerner, L. E. *J. Am. Chem. Soc.* **1993**, *115*, 9201.